考虑储能参与多种辅助服务的主动配电网规划研究

Active Distribution System Planning Considering Energy Storage Systems Participating in Multiple Ancillary Services

(申请清华大学工学硕士学位论文)

培 养 单 位 ： 清华-伯克利深圳学院

学　　　科 ： 电气工程

研 究 生 ： 赵 心 怡

指 导 教 师 ： 孙 宏 斌 　教 授

二〇二一年五月

考虑储能参与多种辅助服务的主动配电网规划研究

赵心怡

Active Distribution System Planning Considering Energy Storage Systems Participating in Multiple Ancillary Services

Thesis Submitted to

Tsinghua University

in partial fulfillment of the requirement

for the degree of

Master of Science

in

Electrical Engineering

by

Xinyi Zhao

Thesis Supervisor: Professor Hongbin Sun

May, 2021

学位论文指导小组、公开评阅人和答辩委员会名单

指导小组名单

孙宏斌	教授	清华大学
沈欣炜	研究科学家	清华大学

公开评阅人名单

张璇	助理教授	清华大学
梁亮	助理教授	哈尔滨工业大学

答辩委员会名单

主席	许银亮	副教授	清华大学
委员	吴文传	教授	清华大学
	郭庆来	教授	清华大学
	郭烨	助理教授	清华大学
	张璇	助理教授	清华大学
秘书	骆哲	助理研究员	清华大学

关于学位论文使用授权的说明

本人完全了解清华大学有关保留、使用学位论文的规定，即：

清华大学拥有在著作权法规定范围内学位论文的使用权，其中包括：（1）已获学位的研究生必须按学校规定提交学位论文，学校可以采用影印、缩印或其他复制手段保存研究生上交的学位论文；（2）为教学和科研目的，学校可以将公开的学位论文作为资料在图书馆、资料室等场所供校内师生阅读，或在校园网上供校内师生浏览部分内容；（3）按照上级教育主管部门督导、抽查等要求，报送相应的学位论文。

本人保证遵守上述规定。

作者签名：赵心怡　　　　　导师签名：孙家诚

日　　期：2021年5月25日　　日　　期：2021年5月25日

摘　要

储能系统因其具备在电源和负载间灵活切换的能力而备受关注。合理的储能选址定容可以增强电力系统的可靠性，延缓其他配电设备的升级需要。此外，储能能够通过循环充放电提供多种辅助服务：较大较慢的充电循环用于提供能量套利，而较小较快的充电循环则用于响应频率调节。通过提供辅助服务，储能系统在电网经济运行上表现出巨大潜力，从而增强了其在配电系统规划中的重要性。

另一方面，储能衰减可能会严重损害储能系统的盈利能力。要解决此问题，我们需要优化储能系统的日常运行以减轻电池老化，延长使用寿命。然而在大多数考虑辅助服务的配电系统规划模型中，此问题难以得到解决，因为在长期规划中纳入快速变化的储能系统实时信号用以响应辅助服务，计算任务繁重。

因此，本文针对具有储能的配电系统提出了确定性和两阶段随机规划的扩建方案，考虑了储能衰减和其提供辅助服务带来的收益。这两种规划方法均采用混合整数线性模型，优化了配电系统规划总成本：包括投资运维成本，电力交易成本以及储能的调频收益。为了避免储能参与调频过程中的过充、过放，在目标函数里增加了一个衰减罚项，可有效延长其使用寿命，提高储能盈利能力。分章小结如下：

首先，对配电系统的确定性规划和两阶段随机规划进行了对比分析，突出了两阶段随机规划在考虑不确定性后的计算难度，由此引出两种经典的解决方法：L 形算法和渐进对冲算法。本章的算法模型介绍，为后续章节奠定了理论基础。

其次，提出了一种考虑储能的配电系统最优规划方法，其网络重构，储能选址定容，及变电站扩建在一个混合整数模型中得到优化。在系统运行阶段，目标函数共同优化了储能衰减和其提供辅助服务收益两项。算例表明，考虑储能衰减的规划方案可将其寿命延长一年。此外，储能调频收益可与其参与能源套利的收入相当。

最后，本文考虑负荷需求和电价等不确定性，采用高斯混合模型和蒙特卡洛模拟，生成了具有代表性的随机场景。为加速求解，提出了一种改进的渐进对冲算法，实现多场景并行计算。算例表明，在对 33 节点配电系统进行扩建规划时，改进算法计算 100 个场景的效率约为 L 形算法的 15 倍，Gurobi 求解器的 5 倍。此外，设计了四种渐进对冲算法作为对照实验，验证了改进算法的有效性。

关键词：储能系统；辅助服务；衰减罚项；两阶段随机规划；渐进对冲算法

ABSTRACT

Energy storage systems (ESS) are receiving more attention crediting to their ability of flexibly switching between power supply and load demand. Appropriate siting and sizing of ESSs can benefit the system's reliability and postpone the upgrade of other distribution facilities. Moreover, ESSs are capable of providing various ancillary services via cyclic behaviors. Generally, macro charge/discharge cycles play an important role in energy arbitrage, and micro regulation up/down cycles respond to the requirement of frequency regulation. By providing multiple ancillary services, ESSs have great potential in improving the economy of the power grid, which strengthens its importance for distribution system planning.

On the other hand, degradation may harm ESS profitability significantly. To fix it, we need to optimize the daily operation of ESS to mitigate the aging process and prolong its lifespan. However, this issue was not addressed properly in most distribution system planning models considering multiple ancillary services. In fact, it is computationally burdensome to incorporate the rapidly changing real-time signals of ESSs in the long-run distribution system planning.

In this dissertation, deterministic and two-stage stochastic programming is proposed for the distribution system with ESSs, where the storage degradation and ancillary service revenue are both considered. Both programs are formulated as mixed-integer linear programming (MILP) that optimizes the overall planning cost, including investment and maintenance cost, power transaction cost, and ESS revenue from regulation services. A degradation penalty is added to the objective to avoid excessive charge/discharge when ESS provides regulation services, thus prolonging its lifespan to make more profits. The outline of each chapter can be concluded as follows:

First, a systematic review of deterministic and stochastic linear programs for distribution system planning is presented. It is shown that with consideration of uncertainties, two-stage stochastic programming is much more complicated than deterministic programming. Two classical decomposition techniques, e.g., the L-shaped method and the progressive hedging algorithm, are introduced with their pseudo-codes, laying a theoretical foundation for the solution method proposed in later sections.

Second, an optimal planning method is proposed for a distribution system with ESSs, where the network configuration, siting and sizing for ESSs, and substation expansion, are optimized via a MILP model. During the operation stage, ESS degradation and its revenue from ancillary service provision are co-optimized in the objective. In the case study, the planning result demonstrates that considering the degradation penalty can extend ESS lifespan by one year. And, the revenue from ESSs by providing regulation services is comparable with that of energy arbitrage.

Finally, uncertainties of load demand and electricity prices are taken into account. A Gaussian mixture model is adopted to characterize these uncertainties and a set of representative scenarios are sampled. To accelerate the optimization, a modified progressive hedging (PH) algorithm with parallel computing is introduced. It is demonstrated through a 33-bus distribution system that the proposed algorithm reaches a speed approximately 15 times as fast as the L-shaped method and 5 times of the Gurobi solver in 100 scenarios. The effectiveness of every algorithmic enhancement of the modified PH on the basic PH is also demonstrated via the four designed PH algorithms.

Keywords: Energy storage system; ancillary service; degradation penalty; two-stage stochastic programming; progressive hedging algorithm

TABLE OF CONTENTS

LIST OF FIGURES AND TABLES

LIST OF SYMBOLS AND ACRONYMS

Abbreviations:

INV	Investment
MAT	Maintenance
eL	Existing line
nL	Candidate new line
SUB	Substation
ESS	Energy storage system
PT	Power transaction
LMP	Locational marginal price
REG	Regulation services
SOC	State of charge
deg	Degradation
cur	Load curtailment
RES	Renewable energy source
CAISO	California independent system operator
LIB	Lithium-ion battery
DG	Distributed generator
IESP	Integrated energy service provider
DSEP	Distribution system expansion planning
MILP	Mixed-Integer linear programming
GMM	Gaussian mixture model
PH	Progressive hedging
DSO	Distribution system operator
MCS	Monte Carlo simulation
PDF	Probability density function
MISOCP	Mixed-Integer second-order cone programming
FW-PH	Frank-Wolfe progressive hedging

Sets:

Ψ_{eL}	Set of existing lines
Ψ_{nL}	Set of candidate new lines

Ω_{SUB}	Set of substation candidate nodes
Ω_{ESS}	Set of ESS candidate nodes
Ω_D	Set of load nodes

Indices:

j	Index of the jth existing line
k	Index of the kth new line
z	Index of new line option
b	Index of new substation option
e	Index of ESS option
i	Index of planning year
t	Index of hour in a day
l	Index of load node
m	Index of substation node
n	Index of ESS node
α	Index of season
s	Index of stochastic scenario

Parameters:

γ	Annual discount rate
C, O	Unit cost of investment/maintenance
T	Total number of hours
S	Total number of scenarios
θ_α, θ_s	Probability of season α/scenario s
Γ	Total node number of the distribution system
W^{LMP}	Locational marginal price [\$/MWh]
$W_{\text{REG}}^{\text{up}}, W_{\text{REG}}^{\text{dn}}$	Regulation up/down service price [\$/MWh]
M_{cur}	Penalty for load curtailment
M_{deg}	Penalty for ESS degradation
M	Penalty factor for the Big-M method
φ	Vector of ESS degradation multipliers [MW^{-1}]
Ξ^{eL}	Node-branch incidence matrix for existing lines
Ξ^{nL}	Node-branch incidence matrix for new lines
D	Load demand [MWh]
$\omega^{\text{up}}, \omega^{\text{dn}}$	Proportion of ESS capacity committed to regulation up/down services
Z^{eL}	Impedance of each existing line [Ω]

X

Z^{nL}	Impedance of each new line [Ω]
$\sigma^{\mathrm{up}}, \sigma^{\mathrm{dn}}$	Standard deviation of regulation up/down signals
F_{max}	Maximum of branch current [p.u.]
$E_{max}^{\mathrm{SUB}}, E_{max}^{\mathrm{ESS}}$	Maximum of substation/ESS capacity [MWh]
P_{max}	Maximum of ESS power output [MW]
E_0	Initial value of ESS state of charge [MWh]

Decision Variables:

x	Planning decision on lines, substations and ESSs
y	Operating decision on lines, substations and ESSs
p^{SUB}	Power from the bulk power system [MWh]
$r^{\mathrm{up}}, r^{\mathrm{dn}}$	ESS committed capacity for regulation up/down service [MW]
β^{ESS}	Vector of ESS operation decision variables
d^{cur}	Load curtailment [MWh]
f^{eL}	Branch current of existing line [p.u.]
f^{nL}	Branch current of new line [p.u.]
$p^{\mathrm{ch}}, p^{\mathrm{dis}}$	ESS charge/discharge power [MW]
ξ^{SOC}	ESS state of charge [MWh]
u	Node voltage [p.u.]
$\chi^{\mathrm{up}}, \chi^{\mathrm{dn}}$	Ancillary variables in the Big-M method

CHAPTER 1 INTRODUCTION

1.1 Background and Motivation

Despite that the global power demand declined by 2% due to the Covid-19 pandemic last year[1], the Chinese load demand still kept going up. With the recovery of the global economy, it is expected that the overall power demand will restore a fast-growing trend. Considering the goal of carbon neutrality, future power systems ought to accommodate rising shares of renewable energy sources (RES). The intermittent nature of RES poses significant challenges to the balance between load and generation in real time. To cope with these challenges, one solution is to install energy storage systems (ESS) for the purpose of shifting the peak load[2] and benefiting the renewable penetration[3]. Batteries have been more and more economical[4] and are proved to have a startling decline speed in levelized cost of energy[5]. Such that, ESSs have reached widespread application in distribution systems, e.g., as an effective means of energy arbitrage.

With the development of energy storage technologies, the application of ESSs in distribution systems is no longer limited to arbitrage or load leveling[6-7]. These storage units play a crucial role in handling voltage drop and power loss while ensuring a high reliability of the distribution system. Considering that ESS's shorter duration applications (mainly less than 4 hours) remain the most cost-effective[8], ESSs are capable of providing multiple ancillary services through charge and discharge, including voltage support, loss reduction, reserve procurement, congestion alleviation, network expansion deferral, and so on. As a matter of fact, the potential revenue from extra ancillary services can further improve the profits of ESS investment[9].

To further enhance the cost-effectiveness of ESSs, it is advisable that we should leverage these storage units to provide as many ancillary services as possible when investing in them in power systems[10]. Only then will their benefits overcome the high investment cost. To promote ESS investment, an optimization framework for distribution system planning considering ESSs is supposed to be designed to offer references for practices. This kind of problem is normally constrained by well-defined physical laws such as Kirchhoff's laws and capacity limits to minimize the overall cost or energy loss of the whole

system. Meanwhile, the optimal siting and sizing of all distribution devices will be given in the planning result, which is often represented by integer/binary variables.

Moreover, mitigating the cycle degradation is another way to improve ESS's profitability, which requires the co-optimization of a set of battery behaviors including charge and discharge[9]. In general, the frequency and the depth of discharge of battery cycles vary from one ancillary service to another. For example, when providing frequency regulation services, battery charges with frequent micro-cycles, while participating in energy arbitrage, the cycle tends to have low frequency and high depth of discharge. Various battery cycles also reflect different aging rates. A degradation model which indicates the aging process of multiple ancillary services is needed to be incorporated in the above-mentioned optimization problem, thus co-optimizing the battery behaviors to determine which ancillary service to be provided at a time.

Motivated by these factors, it is imperative to make thorough studies of a distribution system planning model considering ESS providing multiple ancillary services and its degradation. This model can promote the adoption of these storage devices in existing power systems. The dissertation focuses on utilizing mixed-integer programming to illustrate the planning problem and comes up with a novel modified algorithm to accelerate the solution. ESSs providing ancillary services and its degradation model are creatively combined to distribution planning, which could help the system operator improve the economy of the distribution system.

1.1.1 Ancillary Service Market
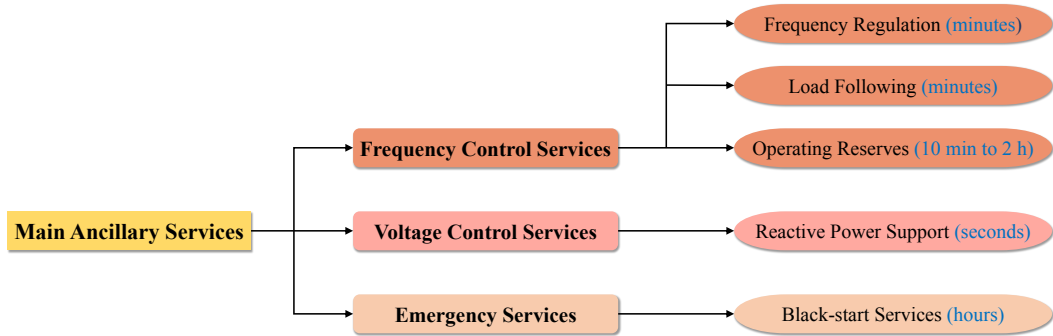
Figure 1.1   Definitions of major types of ancillary services.

Ancillary services garner our interests because of their importance to the reliable and safe operation of power systems. Some of them are under strict control of the government and system operators[11], while others can be procured by bidding among third parties.

Considering that energy markets are different all over the world, it is unreasonable to hold unified standards for these services when they are used for different power systems. In general, main ancillary services can be divided into three types as illustrated in Fig. 1.1 according to their functions.

For a power system, it is extremely important to stabilize the frequency within a certain range to ensure that all devices work safely, and frequency control services can be grouped into three categories. The first one is to provide frequency regulation, which uses generators integrated into the grid to change the active power outputs. For interlinked power grids, the interconnection frequency is controlled via another service, which is load following. The response time of regulation services ranges from seconds to minutes while the load following service handles the frequency deviation over a longer time scale. The third type of frequency control services are spinning and non-spinning operating reserves, which are prepared for fast load restoration after an outage. To cope with different contingency events in the system, ten-minute reserves and thirty-minute reserves are deployed via online and off-line generation units and interrupted loads[12].

Voltage control is also indispensable for power system operation since low voltage can result in severe blackouts[13]. Multiple devices such as generators, synchronous condensers, and capacitor banks can provide or absorb extra reactive power to maintain node voltage within a security scope. Beyond this, once the power fails, emergency services, i.e., black-start service should help the grid resume normal work as soon as possible to reduce economic loss. The provision of this service calls for power plants with enough real and reactive power output which can restart other generation units in the power system.
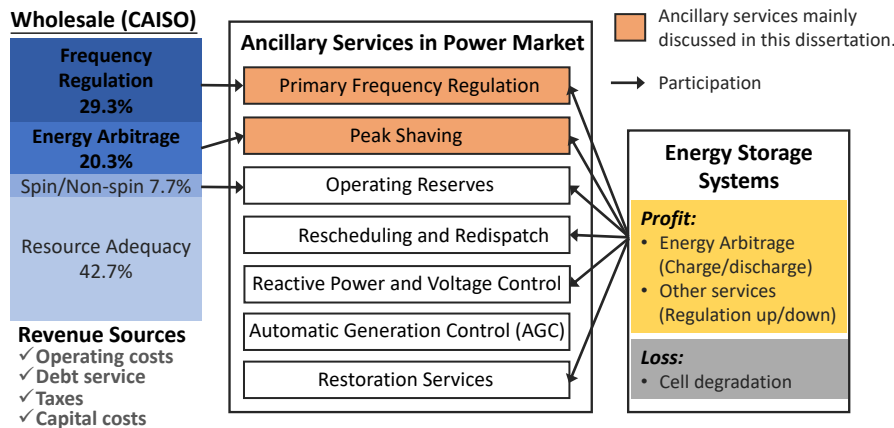
Figure 1.2　Overview of the relationship between power ancillary service market and ESSs.[①]

---

① Data Source: Lazard's Levelized Cost of Storage Analysis Version 4.0

After introducing main ancillary services and their functions, we need to figure out how much benefit they can bring to the current power market. As illustrated by Fig. 1.2, in the wholesale market, e.g., the market operated by the California Independent System Operator (CAISO), a large proportion of its revenue consists of energy arbitrage and frequency regulation[8], both of which can be provided by ESSs. Similarly, for a distribution system, these storage units also play a positive role in enhancing the grid reliability by supplementing multiple ancillary services[14]. Besides, the ESSs' ability of peak load shaving can postpone the upgrades of electric installations[15] thus cutting down the expenses during the planning process[16]. Nevertheless, the feasibility of ESS's profiting from ancillary service products[17] still needs further exploration within a distribution system scale, among which the battery aging problem should not be neglected. For instance, the degradation process of lithium-ion batteries (LIB) is complex. Therefore it used to be described by a nonlinear model that is typically entangled to both stress cycles and operating time[18], which poses great challenges to distribution system planning equipped with LIBs.

1.1.2 Energy Storage System
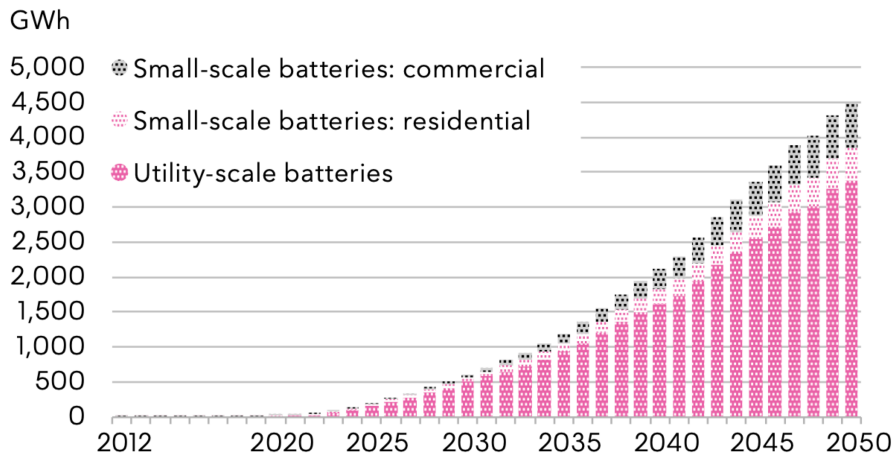
Figure 1.3   Global cumulative battery storage energy capacity.[②]

As mentioned before, ESSs have been central components to power grids crediting to their capability of dynamically switching between power generation and load[19]. In essence, stacked batteries connect in series and parallel to work as a storage system, so the development of ESSs relies on the progress of battery technology. As the technol-

---

② Data Source: BloombergNEF New Energy Outlook 2020 - Executive Summary

ogy becomes mature and the cost is plummeting, it is witnessed last years that battery deployment keeps increasing all over the world, as shown by Fig. 1.3.

So far, wildly used lead-acid batteries have been gradually replaced by more advanced batteries in power system applications. Emerging technologies including the Nickel Cadmium, Sodium Sulphur, Lithium-Ion, and Zinc Bromine batteries are making their way into our grids[20]. Specifically, the LIB is the most promising candidate because of its high energy density and efficiency in practice while others remain in the experimental stage. Design and material are two key factors that determine battery characteristics: capacity, efficiency, cost, life span, energy density, and self-discharge. Fig. 1.4 gives us six common examples of batteries and their feature indices. In practice, ESSs composed of batteries are supposed to strike a balance between high efficiency and low cost hence prospective to commercial usage.

Battery Type	Largest Capacity (Commercial Unit)	Efficiency & Cost	Life Cycle & Depth of Discharge	Energy Density & Self-discharge Rate
Lead Acid (flooded type)	10 MW/40 MWh	• η=72-78%; • 50-150 Euro/kWh	1000–2000 cycles at 70% depth of discharge	✓ 25 Wh/kg; ✓ Self-discharge 2–5%/month
Lead Acid (valve regulated)	300 kW/580 KWh	• η=72-78%; • 50-150 Euro/kWh	200–300 cycles at 80% depth of discharge	✓ 30–50 Wh/kg; ✓ Self-discharge 2–5%/month
Nickel Cadmium (NiCd)	27 MW/6.75 MWh	• η=72-78%; • 200–600 Euro/kWh	3000 cycles at 100% depth of discharge	✓ 45–80 Wh/kg; ✓ Self-discharge 5-20%/month
Sodium Sulphur (NaS)	9.6 MW/64 MWh	• η=89%	2500 cycles at 100% depth of discharge	✓ 100 Wh/kg; ✓ No self-discharge
Lithium-Ion	100MW/129MWh	• η≈90%; • 700-1000 Euro/kWh	3000 cycles at 80% depth of discharge	✓ 90–190 Wh/kg; ✓ Self-discharge 1%/month
Zinc Bromine	1 MW/4 MWh	• η=75%; • 360-1000Euro/kWh	1300 cycles at 100% depth of discharge	✓ 70 Wh/kg; ✓ Negligible self-discharge

Figure 1.4   Characteristics of six typical battery technologies.

Another crucial challenge for battery technology is cell degradation during operation. Batteries will fail to satisfy the peak load demand anymore after chronic capacity decay[21]. It raises the interest to co-optimize the degradation mechanism of batteries in the grid planning problem[9], otherwise, the early retirement of ESSs will harm the economy of the whole power system.

Most batteries have a nonlinear degradation curve where their aging process is divided into calendar aging and cycle aging[22-23]. The former has nothing to do with battery charge or discharge but only with time; the latter refers to the cell degradation caused by cycling behaviors[18]. The degradation rates of batteries are not confined to external factors like time, charge/discharge, and temperature, such that it is extremely hard to obtain a cell degradation model and incorporate it into optimization.

1.1.3 Distribution System Planning

Attributing to its proximity to the load side, the distribution system deserves prior consideration within the whole power system. The investment of the distribution system usually accounts for 30%-50% of the total system cost[24], which renders the necessity of fast and economical planning solutions through optimization models. For distribution system planning, the ultimate goal is to satisfy the increasing load demand while ensuring economical, reliable, and safe operations.

The major tasks of traditional power system planning are the siting and sizing for substations and network reconfiguration. However, we are bound to minimize the adverse effects of newly integrated devices, e.g., energy storage, electric vehicles, distributed energy resources, during the planning process. The concept of the active distribution network appears and promotes the development of the distribution system planning model. More uncertain factors and complicated operation scenarios are taken into account hence give rise to more novel optimization algorithms.

The general workflow for distribution system planning is demonstrated by Fig. 1.5. The planning model should consider both the planning requirement and optimization targets. Besides, power generation planning is an extremely important section of the whole planning problem, including the siting and sizing for substations, distributed generators (DG), and ESSs. Network planning is another important section of the model formulation aiming to minimize the annual investment and operation cost under power balance constraint, line capacity constraint, node voltage limit, network radiality constraint, etc. To take the reliability of the system into account, load curtailment cost, unserved energy cost, and outage cost are also added to the objective function. Moreover, reliability indices such as customer interruption duration (CID), the loss of load probability (LOLP), and the expected energy not supplied (EENS) are engaged into constraints to ensure the network configuration being reliable.

A planning model under activation management is proposed in line with the development trends of smart grids, i.e., DGs, ESSs, and demand response have become increasingly important. Meanwhile, after the reform of electric markets, more stakeholders, e.g., integrated energy service providers (IESP) and some prosumers, are involved in the decision of distribution system planning. To achieve a trade-off between the IESPs' revenue and the total cost spent by system operators, multi-objective planning and multi-layer optimization are used. Furthermore, the scenario and relevant parameters are more com-

Spatial load forecasting and analysis of current grid in the planning area

Model formulation

✓ Power generation planning: siting & sizing for substations/ESSs/ EV charging stations.
✓ Network planning: network configuration; sizing for feeders.
✓ Planning under active management: siting & sizing for DGs.
✓ Planning considering multi-stakeholders: distribution system operators & integrated energy service providers.

Planning structures

- Multi-object planning;
- Two-layer optimization method;
- Planning considering uncertainties;
- Multi-stage planning.

Solution methods

➢ Optimization algorithm:
  1. Branch & bound;
  2. Benders decomposition;
  3. ……

➢ Artificial-intelligence algorithm:
  1. Genetic algorithm;
  2. Particle swarm optimization;
  3. Simulated annealing algorithm;
  4. ……

The optimal planning scheme for a distribution system is obtained

Figure 1.5   Flowchart of distribution system planning.

plicated accounting for the increasing number of investors, which encourages us to take uncertainties into account. At last, multi-stage planning is utilized especially when the planning period would last for over a decade.

In most cases, there are plenty of binary and integer variables in the objective and constraints of the planning problem. Both optimization algorithms and heuristic algorithms are proposed to accelerate the solution. The former tends to obtain the solution with a lower optimality gap, while the latter can handle a large-scale optimization with higher efficiency.

1.2 Literature Review

A large body of the literature lies in modeling ESS degradation. To estimate ESS's lifespan, semi-empirical battery degradation models[18,25] have been proposed and ap-

plied to predict long-term cycle aging of large-format cells[26]. However, in combination with rainflow uncertainty[27], these models will add excessive computational burden to an optimization scheme. In this regard, there have been several attempts to derive a simplified degradation model and evaluate ESS's profitability. Foggo et al.[9] co-optimizes a data-driven linear penalty term denoting the battery degradation rate in the objective, which maximizes the total revenue of ESSs with energy arbitrage and ancillary services. Cardoso et al.[28] linearizes the function of storage capacity loss within specific domains and considers battery aging effects by a linear constraint. He et al.[29] embeds the calculation of battery cycle life into a profit maximization model for optimal bidding and operational schedules. Based on case studies of a battery and transformer deployment, Xi et al.[30] co-optimizes four types of services provided by the ESS, namely, energy arbitrage, regulation service, restoration service, and transformer load relieving, which are applicable to the utility's transformer capacity planning with batteries. However, the trade-off between the ESS degradation and the income from these ancillary services is ignored in the model. Apart from the above-mentioned literature, a classification of major researches relevant to ESS degradation is listed in Table 1.1. To the best of our knowledge, distribution system expansion planning (DSEP) which considers both ESS's providing ancillary services and its degradation is rarely studied so far.

Table 1.1   Review of literature related to ESS degradation (AS: ancillary service).

Motifs	Methods & Algorithms
ESS degradation & AS [9] [18] [29] [31-32]	Semi-empirical battery degradation model; Profit maximization model; Performance-based regulation mechanism; Rainflow cycle-counting algorithm.
DSEP & ESS degradation [33-36]	Piecewise linearized battery lifetime model; Planning-operation co-optimization model; Mixed-integer linear programming; Benders decomposition.
DSEP & ESS degradation & AS[30]	Failure threshold of ESS capacity; Stochastic dynamic programming model; Dynamic programming algorithm.

Among studies on optimization for DSEP, convex relaxation[37] combined with *DistFlow*[38] has been a popular method although it is not easy to guarantee an exact relaxation. Mixed-integer linear programming (MILP) is an alternative, which can be efficiently solved by current commercial optimization solvers and applicable to bidirectional

power flow problems[39]. Besides, considering inherent uncertainties of a realistic distribution system including resource availability, price fluctuations, load change, and policy restrictions, MILP can be further coupled with robust or stochastic optimization. Chen et al.[33] illustrates the uncertainties of PV output and multi-load demand with dual norms to calculate the worst cases directly, then a two-stage robust optimization model for energy hub planning and operation is merged into a single-stage MILP. Baringo et al.[40] considers both short-term and long-term uncertainty in the DSEP, which are handled by the K-means clustering technique and confidence bounds, respectively. Zhou et al.[41] presents a two-stage stochastic programming model, in which Monte Carlo simulation (MCS) is utilized for addressing energy demand and supply uncertainty. Rafinia et al.[42] models multiple uncertainties due to load fluctuations, power generation of wind and solar farm, along with generation deficiency. Stochastic scenarios are generated by a combined process of MCS, Roulette wheel mechanism, and scenario reduction algorithm. However, for every uncertain parameter in these aforementioned DSEP models, the corresponding scenarios are sampled from a single normal distribution. To deal with uncertainty in this dissertation, we adopt a Gaussian mixture model (GMM)[43] which can form smooth approximations to arbitrary probability density functions (PDF).

Moreover, considering uncertainties may lead to excessive computational burden in DSEP problems. As for the stochastic programming framework, decomposition techniques are used to address the tractability issue, and are divided into two categories[44]. One is time-stage-based, known as the L-shaped method, while the other is scenario-based, i.e. progressive hedging (PH).

In fact, the L-shaped method can be considered as a further extension of Benders decomposition for stochastic programming[45]. In 1969, it has been introduced as Van Slyke and Wets's method[46], which is 20 years earlier than the PH idea proposed by Rockafellar and Wets in 1991[47]. The basic rule of the L-shaped method is to replace the nonlinear recourse function in the *master problem* with a lower bound variable, and then approximate the nonlinear term by reformulating the scenario subproblems[48]. This decomposition technique has a broader application in vehicle routing problems[49-50] rather than DSEP.

As for the PH algorithm, it provably converges linearly for stochastic programming with continuous decision variables[51], which is superior to the L-shaped method, since the latter has a significantly increasing difficulty in calculating the *master problem* as the

number of iterations grows[44]. When applied to power system planning, Liu et al.[52] develops the PH algorithm to solve a scenario-based multi-stage stochastic planning model. However, a pipeline model is used to avoid binary variables; thus it is not applicable for the siting and sizing of other facilities in DSEP. Munoz et al.[53] designs planning schemes for a transmission system that considers discrete and continuous decision variables denoting transmission and generation investments, respectively. A hedging process is utilized to resolve decision conflicts in the first stage of large-scale DSEP with scenario uncertainty[54], but it is solved by an evolutionary algorithm. None of these works have modified the PH algorithm to accelerate its convergence when solving a large-scale MILP, which is typical of the DSEP model.

1.3 Gaps and Challenges

Despite ESSs can bring great potential revenue to our distribution systems, there are still significant challenges that have not been settled properly in current ESS planning problems. One of the most imperative tasks is to enhance the accuracy of the ESS's value estimation. To this end, considering the battery cycle degradation during the operation stage is supposed to avoid overestimation of ESS profitability. On the other hand, uncertainty such as the fluctuation of electricity prices should also be taken into account for it can affect ESS profits from ancillary service provision. After incorporating both the degradation model and uncertainty in the planning, we also need to account for the trade-off between the computation efficiency and model complexity.

1.3.1 Modeling of Battery Degradation

In previous works, the modeling of battery degradation designed for optimization mainly utilized cycling parameters to predict the battery cycle life: Shen et al.[55] proposed a battery lifespan estimation model based on uniform cycling, then further extended the model to realistic non-uniform profiles. However, the distributions of battery cycling parameters need to be known as a priori knowledge and any decision change of the cycling profile will affect the estimation model. The degradation model of Hamedi et al.[56] was based on the battery use profile, temperature, and battery characteristics. Zhao et al.[57] measured the life loss of lead-acid batteries with the cumulative Ah throughput in a certain period of time. Most of these papers associate the battery degradation with ESS charge/discharge, state of charge (SOC), and depth of discharge, but few of them con-

sider the degradation resulted from providing ancillary services, i.e. the frequent regulation up/down can accelerate ESS aging process.

When coupling ESS's regulation up/down with its charge/discharge, the parameter-based degradation model is more complicated. According to the American PJM power market, the regulation signals update every two seconds. In response to these signals, the battery providing ancillary services is supposed to adjust the output around 1800 times in an hour. However, the requirement to charge/discharge is not as frequent as that of the regulation up/down, represented by hourly variables. For a degradation model considering these two types of cycle behaviors, one of the key challenges is to simulate ESS regulation up/down and charge/discharge with a unified time scale.

$$deg_n = \sum_{i=1}^{L_n} f_{DoD}(DoD_i)f_{SoC}(SoC_i)f_{CR}(CR_i) + k_t T. \tag{1.1}$$

Eq. (1.1) illustrates a general degradation rate deg_n of LIB, which is a function of cycles L_n and time T. Here L_n represents the total cycle number and k_t is the battery aging rate. DoD_i, SoC_i, and CR_i denote the depth of discharge, the mean SOC, and the current rate of the ith battery cycle, respectively. To incorporate this degradation function into our distribution system planning model, we need to simplify it for the sake of computational efficiency. The critical task is to linearize the function and transfer it into a function of the charge/discharge and regulation up/down behaviors. In this way, we could optimize the battery cycle to mitigate its aging process thus improving ESS profitability.

1.3.2 Uncertainties in Distribution Systems

A stochastic optimization framework is expected to offer a reliable planning scheme since it is robust to the fluctuation of multiple parameters in distribution systems. Stochastic optimization-based planning model has been corroborated capable of reducing the impact of uncertain factors including the demand change, the facility degradation, and the technology advance[58-60]. However, due to massive operation parameters and their complicated interrelationship, most research of distribution system planning only includes limited and simplified representations of uncertain scenarios. To obtain a more comprehensive view of the relationship among these uncertainties, the following challenges remain to be solved:

Insufficient historical data. Historical data of parameters are neither available nor adequate, causing difficulty in defining their probability density functions (PDF). To fix

it, another representation method utilizing a fuzzy membership instead of the probabilistic approach is adopted[61]. Some uncertain parameters are represented probabilistically while others are described possibilistically, rendering a hybrid possibilistic–probabilistic approach[62] as the following.

We assume that the objective of the distribution system planning is $y = f(X, Z)$, where X and Z denote the possibilistic uncertain parameters and probabilistic ones, respectively. They will be modeled by the α-cut method and a scenario-based approach:

- Step 1: The scenario set Ω_s is generated to describe the behavior Z.

- Step 2: The upper bound and lower bound of the α-cut of y is calculated:

$$\underline{y}^\alpha = \min \sum_{s \in \Omega_s} \pi_s \times f(Z_s, X^\alpha);$$

$$\overline{y}^\alpha = \max \sum_{s \in \Omega_s} \pi_s \times f(Z_s, X^\alpha); \tag{1.2}$$

$$X^\alpha \in (\underline{X}^\alpha, \overline{X}^\alpha)$$

- Step 3: Deffuzzify y.

It becomes much more difficult to solve this method which has the deficiency of both pure probabilistic and pure possibilistic methods.

Stochastic dependence. Uncertain factors are usually modeled as time-dependent variables following different Gaussian distributions[63-64]. However, some uncertainties are weakly connected to time but are closely related to other randomness. For instance, the wind power outputs are highly dependent on weather conditions. Therefore, it is necessary to extend the linear dependence to the stochastic dependence of different uncertain factors in distribution systems[65]. In this way, the relationship among multivariate uncertainties should be further investigated and a more advanced probabilistic method is needed to generate stochastic scenarios accurately.

1.3.3 Solution Method

The computation time of a stochastic optimization model scales drastically with the increase of stochastic scenarios. To fix it, decomposition techniques are needed to solve the two-stage stochastic linear program. For the time-stage-based decomposition algorithm, i.e., the L-shaped method, the program is solved based on the iteration between the master problem and subproblem via feasibility and optimality check. Efficient implementations of the L-shaped method work on saving time of solving each subproblem because the solution of subproblems in full scenarios is time-consuming. That is why

recent research proposed to search for an appropriate bunching that can obtain optimal multipliers for several stochastic scenarios at once[66]. However, this research should consider a new bunch in each optimization thus may only apply to solving small-scale stochastic programming.

Efforts were also made on the decomposition of scenarios instead of time stages, namely scenario-based decomposition. One of the representatives is the PH algorithm. However, both the convergence and the solution quality of the PH are sensitive to its penalty factor. Little research in the literature has explored strategies of a variable-dependent penalty factor. With fixed penalty factors, stochastic linear programs especially those with integer variables can be extremely intractable since it is hard to force agreement among all decision variables in the PH process. Cases are that the PH falls into an endless loop and never converges. It still remains elusive on how to effectively detect the PH cyclic behavior and accelerate its convergence.

1.4 Dissertation Overview and Contributions

In this work, a MILP model for distribution systems with ESSs is formulated as a two-stage stochastic programming problem, where ESS degradation is co-optimized in the planning stage. Subsequently, the effects of ancillary service provision by ESSs and uncertainties lying in scenarios are investigated in the solution. Our main contributions are summarized as the following:

- A two-stage stochastic DSEP model that aims at minimizing the overall planning cost is proposed. We leverage a Gaussian mixture model (GMM) to better illustrate the uncertainty observed from historical data for scenario generation instead of directly sampling uncertain parameters from their historical data. Besides, the degradation of ESSs and their revenue on ancillary services are both considered in the distribution system planning.

- To stabilize the solution of two-stage stochastic programming with PH algorithms, we propose to implement *non-anticipativity* constraints by computing a rational average solution instead of the mathematical expectation of the first-stage decision variables. Moreover, with parallel computing process and gap-dependent penalty factors, the modified PH algorithm is further improved in solving the proposed DSEP model. We demonstrate that our modified PH outperforms both the commercial solver Gurobi and the L-shaped method, and prove the effectiveness of

each algorithmic enhancement based on the traditional PH algorithm.
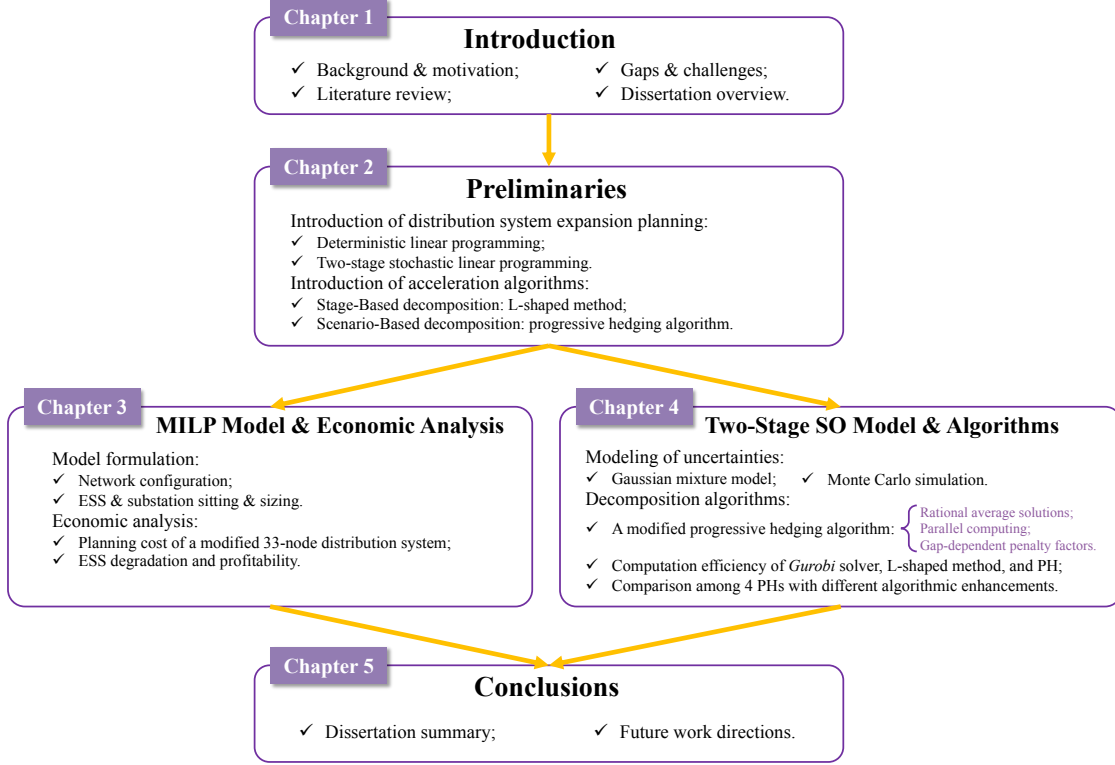
Figure 1.6   An outline of the major parts of this dissertation.

The remainder of this dissertation is organized as Fig. 1.6. Chapter 2 details the preliminaries of the dissertation including an overview of DSEP models and two types of acceleration algorithms. Chapter 3 proposes the mathematical formulation of the deterministic MILP model for the distribution system and the relevant case study. Based on that, Chapter 4 reformulates two-stage stochastic programming to incorporate uncertainties of load demand, electricity prices, and regulation signals. Representative scenarios are generated via GMM, then the modified PH algorithm is introduced and utilized to solve the two-stage stochastic program. The conclusion is drawn in Chapter 5.

CHAPTER 2 PRELIMINARIES

2.1 Overview

In this chapter, we make a systematic review of research on DSEP models, including deterministic linear programming and two-stage stochastic linear programming. The general forms of these two types of programming models are introduced with detailed descriptions of variables used. The two-stage stochastic linear program is proposed based on the deterministic linear model, and is difficult to be solved because the first-stage decision variables must be determined before the realization of random operation scenarios. To take all possible realization into account, a deterministic equivalent program is introduced which utilizes a value function to represent the expectation of the second-stage objectives in all scenarios. By adding this function in the total objective, a more prescient planning scheme can be obtained since we consider the future effect of the first-stage decision from the beginning.

In order to solve two-stage stochastic linear programming more efficiently, comprehensive knowledge of acceleration algorithms is provided in this chapter. Generally, these algorithms can be divided into stage-based and scenario-based decomposition methods. Based on the expression of the deterministic equivalent program, we detail the implementation of two classical decomposition-based algorithms, the L-shaped method, and the PH algorithm, by pseudo-code. The L-shaped method is a vertical decomposition technique that separates the solving process of the first-stage master problem and the second-stage subproblem into different steps. The PH algorithm is a horizontal decomposition method where both the first-stage and the second-stage decision variables are solved in each scenario. We then present a modification of the PH algorithm as one of our main contributions. The background information of these decomposition methods lays the foundation for our modified PH proposed in the following section.

2.2 Distribution System Expansion Planning

To cope with the increasing load demand and high renewable penetration, more and more distribution facilities like feeders, substations, and ESSs ought to be added to our

distribution systems which were built decades ago. To determine the location, capacity, and operation time for these facilities, an important optimization model named DSEP is proposed to support the decision-making of system operators. In most cases, the objective of a DSEP consists of the investment cost, maintenance cost, and power purchasing cost. Sometimes, the decision-maker will take other factors such as carbon emission and energy loss into account, which will be discounted as cost and added to the objective. In addition, some penalty terms will also be included in the objective function to avoid adverse situations, i.e., power curtailment in the grid.

2.2.1 Deterministic Linear Programming

The general form of a deterministic linear program for power distribution system planning is

$$\min z = c^T x$$

$$\text{s.t. } Ax = b, \tag{2.1}$$

$$x \geq 0,$$

where x represents an n-dimensional decision variable, whose value will be determined by solving this constrained optimization problem. A, b, and c are parameters with $m \times n$, $m \times 1$, $n \times 1$ dimensions. The objective function $\min z = c^T x$ denotes the minimization of the total cost spent for the distribution system. Besides, constraints are another important part of the program which can be divided into two types: the simple non-negative requirement for decision variables $x \geq 0$, and important physical limits represented by $Ax = b$. Actually, there are both equality and inequality constraints involved in the distribution system planning, i.e., power balance limit is equality and capacity limit is inequality constraint. By introducing *slack variables*, all inequalities can be reformed as equality ones:

$$a_i x \leq b_i \text{ becomes } a_i x + s_i = b_i. \tag{2.2}$$

Here s_i is the non-negative slack variable whose coefficient is regarded as zero in the objective function. In this way, all these constraints can be represented by a large linear matrix equality $Ax = b$.

To solve this linear program, our target is to find a specific value for the decision variable x. A feasible solution is supposed to meet all constraints listed. Usually, there is one optimal solution x^* that satisfies the constraint set and $c^T x^* \geq c^T x$. Some programs could be infeasible without feasible solution or unbounded with the feasible region

extending to infinity.

When performing sitting and sizing for multiple distribution facilities, a large number of binary decision variables should be introduced. It transforms the DSEP to mixed-integer programming. Assuming that there are numerous investment collections of feeders, substations, and ESSs, we need to check all their feasibility to ensure the specific investment scheme can satisfy the constraint set at any time. After that, we need to pick the optimal scheme with the lowest objective from all feasible solutions. With the following notations:

$$x_j = \begin{cases} 1 & \text{if distribution facility } j \text{ is built,} \\ 0 & \text{otherwise,} \end{cases} \tag{2.3}$$

and

$$c_{1i} = \text{cost of using distribution facility } i, \tag{2.4}$$

the DSEP model is illustrated by the following MILP:

$$\min z = \sum_{i=1}^{n} c_{1i} x_i + c_2^T y$$

$$\text{s.t. } \sum_{i=1}^{n} a_{1i} x_i + A_2 y \le b, \tag{2.5}$$

$$x_i \in \{0, 1\}, y \ge 0.$$

When A_2 equals zero and the constraint becomes $\sum_{i=1}^{n} a_{1i} x_i \le b$, representing a typical constraint in a DSEP model, to avoid redundant distribution facility built at the same place.

2.2.2 Two-Stage Stochastic Linear Programming

For the sake of reliability and accuracy of planning, a deterministic linear program is no longer practical due to its limitations of fixed parameters. Instead, random variables $\xi = \xi(\omega)$ are introduced to replace those fixed parameters aiming to reflect the uncertainty inherent in future operation scenarios. In this way, specific values of these random variables will only be determined after the realization of a certain stochastic scenario, a.k.a. random experiments[48].

Apart from the classification of integer and constant variables, decision variables are divided into first-stage and second-stage ones under the stochastic setting. The first-stage variable (i.e. the investment of a certain distribution facility) represents the decision made before the random experiment, while the second-stage decision variable (i.e. the power

bought from the bulk power system) is dependent on specific stochastic scenarios. The common notations for the first-stage and second-stage variables are x and $y(\omega)$, respectively. Decision-makers have to determine the first-stage variable x based on their *prior belief*, i.e., which random event ω will happen[51]. Then, the second-stage variable $y(\omega)$ will be solved under this specific event. Based on the event sequence, we have:

$$x \rightarrow \xi(\omega) \rightarrow y(\omega). \tag{2.6}$$

After the introduction of two-stage decision variables, we reformulate the previous linear program in Eq. (2.1) to two-stage stochastic programming[67-68]:

$$\min z = c^T x + E_\xi \left[\min q(\omega)^T y(\omega) \right]$$
$$\text{s.t. } Ax = b, \tag{2.7}$$
$$T(\omega)x + W y(\omega) = h(\omega),$$
$$x \geq 0, y(\omega) \geq 0.$$

In the first stage, x is a decision variable with the dimension of $n_1 \times 1$; c, A, and b are matrices with dimension $n_1 \times 1$, $m_1 \times n_1$, and $m_1 \times 1$, separately; $y(\omega)$ is a n_2-dimensional vector; $q(\omega)$, $h(\omega)$, and $T(\omega)$ are $n_2 \times 1$, $m_2 \times 1$, and $m_1 \times n_1$, respectively. After the random experiment $\omega \in \Omega$, the second-stage decision variable $y(\omega)$ will be disclosed based on the scenario-dependent matrices $q(\omega)$, $h(\omega)$, and $T(\omega)$.

The objective of Eq. (2.7) has two parts: the deterministic first-stage term $c^T x$ and the mathematical expectation of the second-stage objective $q(\omega)^T y(\omega)$ which is also known as the recourse function. Note that this second-stage term will only be determined after the realization of the random variable ω which follows the sequence in Eq. (2.6). We hence rewrite the second-stage objective to

$$Q(x, \xi(\omega)) = \min_y \left\{ q(\omega)^T y | W y = h(\omega) - T(\omega)x, \ y \geq 0 \right\}. \tag{2.8}$$

By defining the expectation of the second-stage objective as

$$\mathcal{Q}(x) = E_\xi Q(x, \xi(\omega)), \tag{2.9}$$

we obtain a *deterministic equivalent program* which stresses the difference from a deterministic linear program on the second-stage value function $\mathcal{Q}(x)$

$$\min z = c^T x + \mathcal{Q}(x)$$
$$\text{s.t. } Ax = b, \tag{2.10}$$
$$x \geq 0.$$

We can only get the exact optimal solution x^* if we know which scenario will be ultimately realized. However, it is still impossible for us to predict the future. Hence we need to compute the expected second-stage value $\mathcal{Q}(x)$ as a result of taking a certain decision x. We consider the future effects of the first-stage decision by adding this term to the final objective, thus reaching a more farsighted planning scheme.

2.3 Acceleration Algorithm

As mentioned in Section 2.2.2, for two-stage stochastic programming, the first-stage decision variable has a long-term effect lasting for the whole planning period and should be taken before the uncertainty is revealed. The short-term second-stage decision variable tends to be affected by the first-stage decision and shows high dependence on random variables in each scenario. Numerous random variables bring significant difficulty to the solution of a two-stage stochastic program. Also, considering too many scenarios in the program makes things worse.

A growing body of literature has emerged to solve this problem. Carøe et al.[69] proposed a generalized L-shaped method to solve stochastic programs with integer recourse. Two cases were utilized to demonstrate the effectiveness of cutting plane techniques and the branch-and-bound algorithm in solving the second-stage problem. Laporte et al.[70] proposed an integer L-shaped method and compared it with Benders decomposition and the classical L-shaped method. The finite convergence and the solution optimality of the proposed method were demonstrated by a two-stage stochastic program whose first-stage decisions are binary. Gade et al.[71] utilized the PH algorithm to solve both two-stage and multi-stage stochastic mixed-integer programming where the solution quality was assessed via computing the lower bound from the PH algorithm. Watson et al.[51] provided four algorithmic innovations of PH algorithms to improve the efficiency of solving a two-stage stochastic program with plenty of integer decision variables in both stages.

In summary, there are two types of acceleration algorithms designed as time-stage-based decomposition and scenario-based decomposition, which can accelerate the solution of two-stage stochastic programming. The most well-known representatives of these two decomposition methods are the L-shaped method and the PH algorithm, respectively.

2.3.1 Stage-Based Decomposition: L-Shaped Method

Based on the formulation showed by Eq. (2.10), the L-shaped method utilizes a linear term θ to replace the recourse function $\mathcal{Q}(x)$ in the master problem, thus reducing the difficulty to obtain the optimal first-stage decision x^{υ} (the superscript υ index the number of iteration). Then, after the feasibility check of x^{υ}, the linear subproblem is solved and its objective will be compared with the linear term θ to evaluate the recourse function. The initial value of θ is usually set as a small enough number. So once the second-stage objective is no larger than the value of θ, the current x^{υ} becomes the optimal solution of two-stage stochastic programming.

$$\text{``L-shaped''}\quad \begin{cases} Ax = b, k = 1, \cdots, K; \\ T_k x + W y_k = h_k, k = 1, \cdots, K; \end{cases}$$

Figure 2.1   Block structure of the two-stage extensive form.

The idea of the L-shaped method was originally proposed by Van Slyke and Wets[46]. The name of *L-shape* denotes the block structure of the two-stage extensive form of Eq. (2.1). Under the assumption that the random vector ξ has $k = 1, \dots, K$ finite realizations, the second-stage decision y_k is matched with $\xi_k = (q_k, h_k, T_k)$ in each random event:

$$\min c^T x + \sum_{k=1}^{K} p_k q_k^T y_k$$

$$\text{s.t. } Ax = b, \tag{2.11}$$

$$T_k x + W y_k = h_k, k = 1, \dots, K;$$

$$x \geq 0, y_k \geq 0, k = 1, \dots, K,$$

where p_k represents the probability of each realization.

Based on the above extension form, the standard L-shaped method can be stated as follows. We define three counting variables: the iteration index r, the optimality cut index

u, and the iteration index v.

Algorithm 1: Standard L-shaped Method.

---

1. **Initialization:** $r = u = v = 0$.
2. **while** $\theta^v < w^v$ **do:** $v \leftarrow v + 1$.
3. $(x^v, \theta^v) \leftarrow \text{argmin}_x (c^T x + \theta)$
4.   s.t. $Ax = b$; $D_f x \geq d_f$, $f = 1, \ldots, r$;
5. $E_g x + \theta \geq e_g$, $g = 1, \ldots, u$; $x \geq 0, \theta \in \mathfrak{R}$.
6.   Set $F = 1$.
7.   **for** $k \in K$ **solve:**
8. $\min_{v^+, v^-} w' = e^T v^+ + e^T v^-$
9.   s.t. $W y + I v^+ - I v^- = h_k - T_k x^v$; $y \geq 0$, $v^+, v^- \geq 0$.
10.   **if** $w' \geq 10^{-5}$ **do:** $F \leftarrow 0$ **break**.
11.   **end if**
12.   **end for**
13.   **if** $F = 0$ **do:** $r \leftarrow r + 1$. $D_r = (\tau^v)^T T_k$, $d_r = (\tau^v)^T h_k$.
14.   Add $D_f x \geq d_f$, $f = 1, \ldots, r$ to the constraint set.
15.   **end if**
16.   **if** $F = 1$
17.   **for** $k \in K$ **solve:**
18. $\min_y w = q_k^T y$
19.   s.t. $W y = h_k - T_k x^v$; $y \geq 0$.
20.   **end for**
21.   Update: $u \leftarrow u + 1$,
22. $E_u = \sum_{k=1}^K p_k (\pi_k^v)^T T_k$, $e_u = \sum_{k=1}^K p_k (\pi_k^v)^T h_k$.
23. $w^v = e_u - E_u x^v$.
24.   Add $E_g x + \theta \geq e_g$, $g = 1, \ldots, u$ to the constraint set.
25.   **end if**
26. **end while**

In Step 5, if there is no such constraint as $E_g x + \theta \geq e_g$ in the linear program, θ^v will be set to $-\infty$ and not be considered in Step 3. $e^T = (1, \ldots, 1)$ in Step 8 is introduced to check the feasibility of a first-stage decision x^v when solving subproblems. τ^v in Step 13 and π_k^v in Step 22 represent the dual multipliers associated with the optimal solution of the linear program in Step 8-9 and Step 18-19, respectively. By iteratively adding feasibility cuts and optimality cuts, both feasible and optimal solution x^v is eventually obtained.

2.3.2 Scenario-Based Decomposition: Progressive Hedging

Another representative decomposition method is the PH algorithm, which was initially utilized to solve programming with continuous decision variables. It was introduced to solve two-stage stochastic programs recently. The PH algorithm has a different decomposition rule from the L-shaped method. If we put the L-shaped method as a vertical decomposition technique since it decomposes stochastic programs by time stages, then

the PH algorithm is definitely a horizontal technique with a scenario-based decomposition process. The latter works as an effective heuristic to solve the stochastic program in each scenario, then the *non-anticipativity* constraint is utilized to promote the scenario-specific solutions to converge on their mathematical expectation.

For notation simplicity, the two-stage extensive form in Eq. (2.11) is reformulated as below:

$$\min c^T x + \sum_{k=1}^{K} p_k q_k^T y_k \tag{2.12}$$

$$\text{s.t. } (x, y_k) \in \mathcal{Q}_k, \ \forall k \in K,$$

where $(x, y_k) \in \mathcal{Q}_k$ denotes the constraint set in each realization. With both integer decision variable x and continuous y_k, some constraints in $\mathcal{Q}_k$ result in the non-convexity of the stochastic program. To fix it, the scenario-dependent copied x_k is introduced to replace the first-stage decision x via the *non-anticipativity* constraint $x_k = x, \forall k \in K$, which ensures x_k must be the same for each scenario.
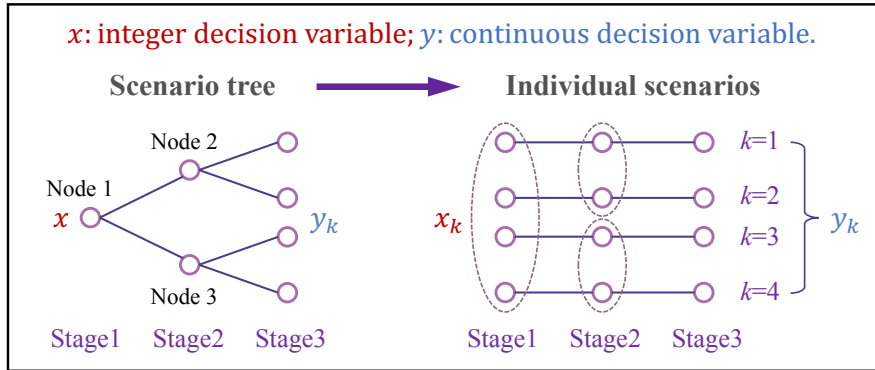
Figure 2.2 Relationship between decision variables at different time stages and different scenarios in the PH process.

We then apply Lagrangian relaxation to the *non-anticipativity* constraint and obtain the following augmented Lagrangian dual function:

$$L^\rho(x, y_k, \bar{x}^{\upsilon-1}, w) := \sum_{k=1}^{K} p_k L_k^\rho(x_k, y_k, \bar{x}^{\upsilon-1}, w_k)$$

$$= \sum_{k=1}^{K} p_k \left(c^T x_k + w_k^{\upsilon-1} \cdot x_k + \frac{\rho}{2} \cdot \|x_k - \bar{x}^{\upsilon-1}\|^2 + q_k^T y_k \right), \tag{2.13}$$

where w denotes the Lagrange multiplier of the *non-anticipativity* constraint. Eq. (2.13) is a fully separable objective function that can be solved individually in each scenario. Fig. 2.2 further illustrates the relationship between decision variables at different time

stages and different scenarios. The basic idea of the PH algorithm is to transform the non-separable optimization into several scenario-based subproblems.

According to Eq. (2.11), **Algorithm 2** is designed to show the decomposition process of the PH algorithm. The positive penalty factor ρ and termination threshold ε are input parameters:

Algorithm 2: Standard Progressive Hedging Algorithm.

---

1. **Initialization:** $v \leftarrow 1, w_s^{v-1} \leftarrow 0, g^v \leftarrow 0, \forall k \in K$.
2. **for** $k \in K$ **do:**
3. $\quad x_k^v \leftarrow \text{argmin}_{x,y_k}(c^T x + q_k^T y_k) \quad$ s.t. $(x, y_k) \in \mathcal{Q}_k$
4. **end for**
5. Update: $\bar{x}^v \leftarrow \sum_{k=1}^K p_k x_k^v$
6. **for** $k \in K$ **do:** $w_k^v \leftarrow w_k^{v-1} + \rho(x_k^v - \bar{x}^v)$.
7. **end for**
8. Update: $g^v \leftarrow \sum_{k=1}^K p_k \cdot \|x_k^v - \bar{x}^v\|$.
9. **while** $g^v \geq \varepsilon$ **do:** $v \leftarrow v + 1$.
10. $\quad$ **for** $k \in K$ **do:**
11. $\quad\quad x_k^v \leftarrow \text{argmin}_{x,y_k}\left(c^T x + w_k^{v-1} \cdot x + \frac{\rho}{2} \cdot \|x - \bar{x}^{v-1}\|^2 + q_k^T y_k\right)$
12. $\quad\quad$ s.t. $(x, y_k) \in \mathcal{Q}_k$
13. $\quad$ **end for**
14. $\quad$ **repeat Step 5-8**.
15. **end while**

2.4 Conclusions

We introduce two widely-used DSEP models in this chapter. The deterministic linear program is one of the most straightforward planning methods. With slack variables, both equality and inequality constraints can be written in a unified form $Ax = b$. To solve this program, we should search for a feasible solution x which results in the lowest objective. Sometimes the integer decision variable is involved in programming which can play a role in sitting and sizing of certain facilities.

Considering that decision making is subject to considerable uncertain factors in a real distribution system, two-stage stochastic programming is adopted. These decision variables can be divided into two types according to the event sequence. The first-stage decision is a common decision vector and is not affected by different realization while the second-stage decision is scenario-specific. The objective of two-stage stochastic programming has both the deterministic first-stage part and the mathematical expectation of second-stage objectives in each scenario. To solve this intractable model formulation,

some acceleration algorithms which can well decompose the whole program have been proposed and modified in recent research.

Among these decomposition methods, two examples are introduced to demonstrate their effectiveness in solving these coupled two-stage linear programs. The L-shaped method utilizes a linear term to represent the second-stage value function, then approaches this term by optimizing the subproblem in the following iterations. On the other hand, the PH algorithm adopts a scenario-dependent copied x_k via the *non-anticipativity* constraint. Then, initial non-separable programming can be transformed into several scenario-based subproblems. Finally, pseudo-codes of these two representative algorithms are given based on the expression of two-stage stochastic linear programming in Section 2.2.2, which is the theoretical foundation of the solution method in Section 4.3.2 and 4.3.3.

CHAPTER 3 DETERMINISTIC PLANNING FOR A DISTRIBUTION SYSTEM WITH ENERGY STORAGE SYSTEMS

3.1 Overview

Siting and sizing of grid-level storage belong to the most crucial components of the distribution system planning since ESSs can improve the renewable penetration as well as postponing the upgrade of other distribution facilities. The flexibility and resilience of power systems will also be enhanced with the integration of large-scale storage units[72]. Furthermore, ESSs take advantage of the electricity price difference between peak and valley load hours in order to make a profit from energy arbitrage[73]. Multiple ancillary services such as frequency control, voltage control, and emergency services are dependent on ESSs, more or less. Based on the above-mentioned advantages of this key facility, we need to make further investigations to ESS profitability before investing in it in our distribution systems.

The degradation of ESS is a key factor to be reckoned with. Recent research has demonstrated that mitigating ESS degradation by reducing charge cycles contributes to longer lifespan and higher profitability[9,74]. Besides, battery aging due to daily operation is also of interest in power system planning. Our ultimate objective is to realize the maximum value of ESSs in real distribution systems.

In this chapter, an optimal planning scheme is proposed for distribution systems where both the ESS degradation and its profitability from ancillary services are co-optimized. In the planning stage, we consider the network configuration, substation expansion, as well as ESS siting and sizing as a MILP model. Our target is to minimize the overall planning costs, including investment and maintenance cost, power transaction cost, revenue from regulation services, and degradation term of ESSs. By adding this degradation term to the objective, ESS charging/discharging due to energy arbitrage and ancillary services is optimized to prolong its lifetime, thus benefit the economy of the distribution system. Eventually, the proposed planning model is testified on a 33-bus distribution system to demonstrate its effect on promoting ESS profitability.

3.2 Objective and Cost-Related Terms

The DSEP considering ESS degradation and regulation services is established as a MILP model, illustrated in Fig. 3.1. The objective includes five expenses within the planning and operation stage. Network configuration, substation expansion, and ESS siting and sizing are decided in the planning stage, where binary variable x determines whether to invest in the facility or not. As for operation, decision variables can be divided into three categories, which are binary variable y denoting the operating lines, substations, and ESSs; continuous variables related to grid operation, i.e. power transmitted by substations $p_{m,b,t}^{\text{SUB}}$; and the continuous vector $\beta_{n,t}^{\text{ESS}}$ related to ESS's behaviors, including the charge/discharge, regulation up/down and SOC.

Figure 3.1 Overview of the MILP model.
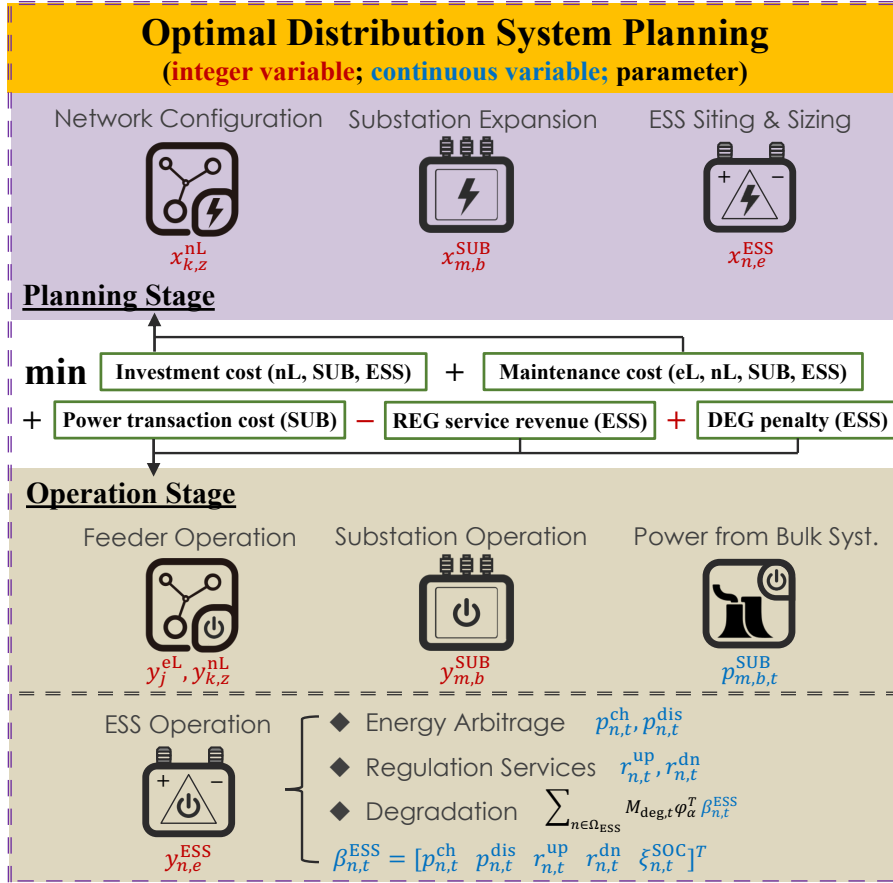
In the planning stage, we assume that the distribution system will invest in lines, substations, and ESSs, whose maintenance fare is also covered in the overall cost. Besides, electricity needs to be bought from a bulk power system as power transaction cost, which will be affected by ESS operation.

Meanwhile, ESSs will provide regulation services to the bulk power system. In this

section, the overall cost of the distribution system is minimized, and the possible revenue of energy arbitrary and frequency regulation services should be considered. To prolong ESS's lifespan, a penalty term relevant to its degradation model is added to the objective function.

3.2.1 Investment Cost

The DSEP includes the investment cost of lines, substations, and ESSs, denoted in Eq. (3.1). Where $x_{k,z}^{\mathrm{nL}}$ is the planning decision of the kth new line with option z, $x_{m,b}^{\mathrm{SUB}}$ is the planning decision of the substation on node m with option b, and $x_{n,e}^{\mathrm{ESS}}$ is the planning decision of the ESS on node n with option e. They are binary decision variables, when $x = 1$ represents the corresponding facility invested in the distribution system and otherwise $x = 0$. $C_{k,z}^{\mathrm{nL}}$, $C_{m,b}^{\mathrm{SUB}}$ and $C_{n,e}^{\mathrm{ESS}}$ are the unit costs to built feeders, substations and ESSs of certain options.

$$
\begin{aligned}
C_{\mathrm{INV}} = &\sum_{k \in \Psi_{\mathrm{nL}}} \sum_{z} C_{k,z}^{\mathrm{nL}} x_{k,z}^{\mathrm{nL}} + \sum_{m \in \Omega_{\mathrm{SUB}}} \sum_{b} C_{m,b}^{\mathrm{SUB}} x_{m,b}^{\mathrm{SUB}} \\
&+ \sum_{n \in \Omega_{\mathrm{ESS}}} \sum_{e} C_{n,e}^{\mathrm{ESS}} x_{n,e}^{\mathrm{ESS}}
\end{aligned}
\tag{3.1}
$$

Note that this work focuses on expansion planning, hence the investment of existing lines will be precluded. Instead, their maintenance cost is considered in Eq. (3.2).

3.2.2 Maintenance Cost

Similarly, the total operation and maintenance cost needs to involve all the components in the distribution network. Where y_{j}^{eL} is the operation decision of the jth existing line, $y_{k,z}^{\mathrm{nL}}$ is the operating decision of the kth new line with option z, $y_{m,b}^{\mathrm{SUB}}$ is the operating decision of the substation on node m with option b, and $y_{n,e}^{\mathrm{ESS}}$ is the operating decision of the ESS on node n with option e. $y = 1$ denotes that the facility is in operation and otherwise $y = 0$. O_{j}^{eL}, $O_{k,z}^{\mathrm{nL}}$, $O_{m,b}^{\mathrm{SUB}}$, and $O_{n,e}^{\mathrm{ESS}}$ are the yearly maintenance costs of existing lines, newly-built lines, substations and ESSs.

$$
\begin{aligned}
C_{\mathrm{MAT}} = \sum_{t=1}^{T} \Big(&\sum_{j \in \Psi_{\mathrm{eL}}} O_{j}^{\mathrm{eL}} y_{j}^{\mathrm{eL}} + \sum_{k \in \Psi_{\mathrm{nL}}} \sum_{z} O_{k,z}^{\mathrm{nL}} y_{k,z}^{\mathrm{nL}} \\
&+ \sum_{m \in \Omega_{\mathrm{SUB}}} \sum_{b} O_{m,b}^{\mathrm{SUB}} y_{m,b}^{\mathrm{SUB}} + \sum_{n \in \Omega_{\mathrm{ESS}}} \sum_{e} O_{n,e}^{\mathrm{ESS}} y_{n,e}^{\mathrm{ESS}} \Big)
\end{aligned}
\tag{3.2}
$$

3.2.3 Power Transaction Cost

To supply the load demand, power is bought from the bulk power system and the cost
is denoted by C_{PT} as below:

$$C_{\text{PT}} = \sum_{\alpha} \theta_{\alpha} \sum_{t=1}^{T} \left(\sum_{m \in \Omega_{\text{SUB}}} W_{\alpha,t}^{\text{LMP}} p_{m,b,t}^{\text{SUB}} \right) \tag{3.3}$$

where $p_{m,b,t}^{\text{SUB}}$ is the power transmitted from substation node m with option b at hour t, θ_{α}
is the portion of typical seasonal scenario α. W^{LMP} denotes the locational marginal price
(LMP).

3.2.4 ESS Revenue of Regulation Services

In real-time operations, revenue will be earned for ESS's providing regulation ser-
vices to the bulk system, denoted as W_{REG}:

$$W_{\text{REG}} = \sum_{\alpha} \theta_{\alpha} \sum_{t=1}^{T} \sum_{n \in \Omega_{\text{ESS}}} \left(W_{\text{REG},\alpha,t}^{\text{up}} r_{n,t}^{\text{up}} + W_{\text{REG},\alpha,t}^{\text{dn}} r_{n,t}^{\text{dn}} \right) \tag{3.4}$$

where non-negative decision variables $r_{n,t}^{\text{up}}, r_{n,t}^{\text{dn}}$ determine how much regulation up/down
capacity is committed. $W_{\text{REG},\alpha,t}^{\text{up}}$ and $W_{\text{REG},\alpha,t}^{\text{dn}}$ represent revenue of ESS providing the unit
capacity for regulation up and down.

3.2.5 Penalty Term of ESS Degradation

In order to trade off between profits earned by ESSs and the battery's cycle degra-
dation cost, a penalty is added in the objective, which consists of two important vectors
shown in Eq. (3.5) and Eq. (3.6). The parameters a_1, a_2 and p_z in (3.5) are constants
relevant to LIB types, which will affect the degradation rates of different ESS's behav-
iors[9]. Besides, $P_{e,\text{max}}$ is the maximum power output of the ESS with option e, which is
normally less than half of its nominal capacity $E_{e,\text{max}}^{\text{ESS}}$. $(\sigma_{\alpha,t}^{\text{up}})^2$ and $(\sigma_{\alpha,t}^{\text{dn}})^2$ are regulation
signal up/down variances at hour t in scenario α. $\omega_{\alpha,t}^{\text{up}}$ and $\omega_{\alpha,t}^{\text{dn}}$ denote the proportion of
ESS capacity committed to regulation up/down services at hour t in scenario α.

$$\varphi_\alpha = \begin{bmatrix} \frac{a_2}{4}(1-p_z) \\ \frac{a_2}{4}(1-p_z) \\ \frac{a_1^2 p_z}{2a_2} y_{n,e}^{\mathrm{ESS}} P_{e,\max}(1.5(\sigma_{\alpha,t}^{\mathrm{up}})^2 - 0.5(\sigma_{\alpha,t}^{\mathrm{dn}})^2 - \omega_{\alpha,t}^{\mathrm{up}}\omega_{\alpha,t}^{\mathrm{dn}}) \\ \frac{a_1^2 p_z}{2a_2} y_{n,e}^{\mathrm{ESS}} P_{e,\max}(1.5(\sigma_{\alpha,t}^{\mathrm{dn}})^2 - 0.5(\sigma_{\alpha,t}^{\mathrm{up}})^2 - \omega_{\alpha,t}^{\mathrm{up}}\omega_{\alpha,t}^{\mathrm{dn}}) \\ 0 \end{bmatrix} \tag{3.5}$$

$$\beta_{n,t}^{\mathrm{ESS}} = \begin{bmatrix} p_{n,t}^{\mathrm{ch}} & p_{n,t}^{\mathrm{dis}} & r_{n,t}^{\mathrm{up}} & r_{n,t}^{\mathrm{dn}} & \xi_{n,t}^{\mathrm{SOC}} \end{bmatrix}^T \tag{3.6}$$

Vector $\beta_{n,t}^{\mathrm{ESS}}$ contains five types of continuous decision variables including the charge/discharge power $p_{n,t}^{\mathrm{ch}}/p_{n,t}^{\mathrm{dis}}$, capacity for regulation up/down $r_{n,t}^{\mathrm{up}}/r_{n,t}^{\mathrm{dn}}$, and SOC $\xi_{n,t}^{\mathrm{SOC}}$, which is related to behaviors of the ESS node n at hour t.

As illustrated in Fig. 3.1, five expenses are involved in the objective shown in Eq. (3.7), with both regulation services and degradation of ESSs taken into account.

$$\begin{aligned} \min \sum_i \gamma^i \Big(& C_{\mathrm{INV}} + C_{\mathrm{MAT}} + C_{\mathrm{PT}} - W_{\mathrm{REG}} \\ & + \sum_\alpha \theta_\alpha \sum_{t=1}^T \sum_{n\in\Omega_{\mathrm{ESS}}} M_{\mathrm{deg},t}\varphi_\alpha^T \beta_{n,t}^{\mathrm{ESS}} \Big) \end{aligned} \tag{3.7}$$

3.3 Kirchhoff's Laws and Network Operational Constraints

This deterministic planning model considers typical constraints for DSEP including Kirchhoff's current law, node voltage limits, and feeders' capacity, which are detailed as below:

$$\begin{aligned} \Xi^{\mathrm{eL}} f_t^{\mathrm{eL}} + \Xi^{\mathrm{nL}} f_t^{\mathrm{nL}} + \sum_{l\in\Omega_D} d_{l,t}^{\mathrm{cur}} + \sum_{m\in\Omega_{\mathrm{SUB}}} p_{m,b,t}^{\mathrm{SUB}} \\ = \sum_{l\in\Omega_D} D_{l,t} - \sum_{n\in\Omega_{\mathrm{ESS}}} \left(p_{n,t}^{\mathrm{dis}} - p_{n,t}^{\mathrm{ch}} + \omega_{\alpha,t}^{\mathrm{up}} r_{n,t}^{\mathrm{up}} - \omega_{\alpha,t}^{\mathrm{dn}} r_{n,t}^{\mathrm{dn}} \right) \cdot (1hr.) \end{aligned} \tag{3.8}$$

$$\left| Z_j^{\mathrm{eL}} f_{j,t}^{\mathrm{eL}} + [\Xi^{\mathrm{eL}}]_{Rowj}^T u_t \right| \le M \cdot (1 - y_{j,t}^{\mathrm{eL}}) \quad \forall j \in \Psi_{\mathrm{eL}} \tag{3.9}$$

$$\left| Z_{k,z}^{\mathrm{nL}} f_{k,t}^{\mathrm{nL}} + [\Xi^{\mathrm{nL}}]_{Rowk}^T u_t \right| \le M \cdot (1 - y_{k,z,t}^{\mathrm{nL}}) \quad \forall k \in \Psi_{\mathrm{nL}} \tag{3.10}$$

$$0 \le d_{l,t}^{\text{cur}} \le D_{l,t} \quad \forall l \in \Omega_D \tag{3.11}$$

$$0 \le p_{m,b,t}^{\text{SUB}} \le \sum_b y_{m,b,t}^{\text{SUB}} E_{b,\max}^{\text{SUB}} \quad \forall m \in \Omega_{\text{SUB}} \tag{3.12}$$

$$|f_{j,t}^{\text{eL}}| \le y_{j,t}^{\text{eL}} F_{j,\max}^{\text{eL}}, |f_{k,t}^{\text{nL}}| \le \sum_z y_{k,z,t}^{\text{nL}} F_{k,z,\max}^{\text{nL}} \quad \forall j \in \Psi_{\text{eL}}, \forall k \in \Psi_{\text{nL}}. \tag{3.13}$$

Based on the linearized network model[75-76], Eqs. (3.8)-(3.10) implement the power balance between the generation and the demand, following Kirchhoff's Laws. The simplified network expression is initially an adapted version of the DC power flow model which used to be applied in the transmission system. However, previous research[3,77-78] has demonstrated the effectiveness of this network model in solving DSEP with acceptable accuracy. Eqs. (3.11)-(3.12) set the upper and lower bound of network-related variables to ensure that all distribution facilities operate within safe ranges. Analogously, the upper bound of feeders is limited in Eq. (3.13), since the potential integration of ESSs may lead to increase current at the end of feeders.

3.4 ESS Operational Constraints

In this section, we assume that the capacity of one ESS can be divided into two parts for the use of energy arbitrage and regulation services[9]:

$$\xi_{n,t+1}^{\text{SOC}} = \xi_{n,t}^{\text{SOC}} - (p_{n,t}^{\text{dis}} - p_{n,t}^{\text{ch}} + \omega_{\alpha,t}^{\text{up}} r_{n,t}^{\text{up}} - \omega_{\alpha,t}^{\text{dn}} r_{n,t}^{\text{dn}}) \cdot (1hr.)$$
$$\forall n \in \Omega_{\text{ESS}}, t = 1, 2, \cdots, 23 \tag{3.14}$$

$$0 \le \xi_{n,t}^{\text{SOC}} \le \sum_e y_{n,e,t}^{\text{ESS}} E_{e,\max}^{\text{ESS}} \tag{3.15}$$

$$(r_{n,t}^{\text{dn}} + p_{n,t}^{\text{ch}}) \cdot (1hr.) \le \sum_e y_{n,e,t}^{\text{ESS}} E_{e,\max}^{\text{ESS}} - \xi_{n,t}^{\text{SOC}} \tag{3.16}$$

$$(r_{n,t}^{\text{up}} + p_{n,t}^{\text{dis}}) \cdot (1hr.) \le \xi_{n,t}^{\text{SOC}} \tag{3.17}$$

$$\omega_{\alpha,t}^{\text{up}} r_{n,t}^{\text{up}} + p_{n,t}^{\text{dis}} - \omega_{\alpha,t}^{\text{dn}} r_{n,t}^{\text{dn}} \leq \sum_{e} y_{n,e,t}^{\text{ESS}} P_{e,\max}^{\text{ESS}} \tag{3.18}$$

$$\omega_{\alpha,t}^{\text{dn}} r_{n,t}^{\text{dn}} + p_{n,t}^{\text{ch}} - \omega_{\alpha,t}^{\text{up}} r_{n,t}^{\text{up}} \leq \sum_{e} y_{n,e,t}^{\text{ESS}} P_{e,\max}^{\text{ESS}} \tag{3.19}$$

$$r_{n,t}^{\text{up}} + p_{n,t}^{\text{dis}} \leq \sum_{e} y_{n,e,t}^{\text{ESS}} P_{e,\max}^{\text{ESS}} \tag{3.20}$$

$$r_{n,t}^{\text{dn}} + p_{n,t}^{\text{ch}} \leq \sum_{e} y_{n,e,t}^{\text{ESS}} P_{e,\max}^{\text{ESS}} \tag{3.21}$$

$$\xi_{n,t}^{\text{SOC}} = \sum_{e} y_{n,e,t}^{\text{ESS}} E_{e,0}^{\text{ESS}}, \quad t = 1, 24 \tag{3.22}$$

$$p_{n,t}^{\text{ch}}, p_{n,t}^{\text{dis}}, r_{n,t}^{\text{up}}, r_{n,t}^{\text{dn}} \geq 0 \tag{3.23}$$

Eq. (3.14) denotes the SOC update rule where we ignore the battery's self-discharge rate and resistive losses during ESS operation. For different options of ESSs, their SOC ought to remain less than the nominal capacity $E_{e,\max}^{\text{ESS}}$ as shown in Eq. (3.15). Furthermore, constraints (3.16)-(3.17) limit the total capacity of ESSs used for providing ancillary services. Even when $\omega_{\alpha,t}^{\text{up}}$ and $\omega_{\alpha,t}^{\text{dn}}$ equal 1, which means the full committed capacity for regulation up/down is put into use, the total ESS operational capacity is still supposed to be less than its SOC. Similarly, constraints (3.18)-(3.21) set the upper bound of ESS power output in real time. Eq. (3.12) guarantees that the battery SOC in the end equals that at the beginning of a typical day. The non-negativity characteristic of all ESS decision variables is stressed in Eq. (3.23).

3.5 Construction Logical Constraints

To avoid building redundant projects on the same node, Eq. (3.24) denotes that only one option of ESSs or substations built on a specific node can be chosen among all candidate choices. Eq. (3.25) denotes that the substation and ESS will not be available ($y = 0$) when they are not constructed ($x = 0$). Otherwise, if the facility has been built ($x = 1$),

its operating variable can be 1 or 0 ($y = 0/y = 1$). Eq. (3.26) guarantees the radiality of the distribution system, where N_{SUB} represents the number of operating substations.

$$\sum_b x^{\mathrm{SUB}}_{m,b} \leq 1, \ \sum_e x^{\mathrm{ESS}}_{n,e} \leq 1 \tag{3.24}$$

$$y^{\mathrm{SUB}}_{m,b} \leq x^{\mathrm{SUB}}_{m,b}, \ y^{\mathrm{ESS}}_{n,e} \leq x^{\mathrm{ESS}}_{n,e} \tag{3.25}$$

$$\sum_{j \in \Psi_{\mathrm{eL}}} y^{\mathrm{eL}}_j + \sum_{k \in \Psi_{\mathrm{nL}}} \sum_z y^{\mathrm{nL}}_{k,z} = \Gamma - N_{\mathrm{SUB}} \tag{3.26}$$

3.6 Constraint Reformulation by Big-M Method

Note $\varphi^T_\alpha \beta^{\mathrm{ESS}}_{n,t}$ in the objective (3.7) results in some computational difficulties due to considering ESS siting and sizing. That is, the binary decision variable $y^{\mathrm{ESS}}_{n,e}$ is multiplied with the continuous variable $r^{\mathrm{up}}_{n,t}/r^{\mathrm{dn}}_{n,t}$, thus the model is no longer MILP.

To this end, we apply Big-M method to reformulate this term, as illustrated in (3.27)-(3.31), where $\chi^{\mathrm{up}}_{n,e,t}$ and $\chi^{\mathrm{dn}}_{n,e,t}$ are two ancillary decision variables and M is a big constant (1e+5). Non-negative variables $\chi^{\mathrm{up}}_{n,e,t}$ and $\chi^{\mathrm{dn}}_{n,e,t}$ are introduced to replace and relax the product of $y^{\mathrm{ESS}}_{n,e}$ and $r^{\mathrm{up}}_{n,t}/r^{\mathrm{dn}}_{n,t}$.

$$\chi^{\mathrm{up}}_{n,e,t} \leq r^{\mathrm{up}}_{n,t}, \chi^{\mathrm{dn}}_{n,e,t} \leq r^{\mathrm{dn}}_{n,t} \tag{3.27}$$

$$r^{\mathrm{up}}_{n,t} \leq \chi^{\mathrm{up}}_{n,e,t} + M \cdot (1 - y^{\mathrm{ESS}}_{n,e}) \tag{3.28}$$

$$0 \leq \chi^{\mathrm{up}}_{n,e,t} + M \cdot y^{\mathrm{ESS}}_{n,e} \tag{3.29}$$

$$r^{\mathrm{dn}}_{n,t} \leq \chi^{\mathrm{dn}}_{n,e,t} + M \cdot (1 - y^{\mathrm{ESS}}_{n,e}) \tag{3.30}$$

$$0 \leq \chi^{\mathrm{dn}}_{n,e,t} + M \cdot y^{\mathrm{ESS}}_{n,e} \tag{3.31}$$

3.7 Case Study

3.7.1 A Modified 33-Bus Distribution System

A 33-bus distribution system[38] has been modified and tested to verify the effectiveness of the proposed method. As shown in Fig. 3.2, these 5 dotted lines are alternatives for building new feeders, and 32 solid ones represent existing lines. In the planning stage, the topology can be changed with some new feeders built and other existing lines abandoned. As mentioned in Section 3.5, no isolated node and loop are allowed in the operation stage, which means only 32 feeders will be operating in the system.
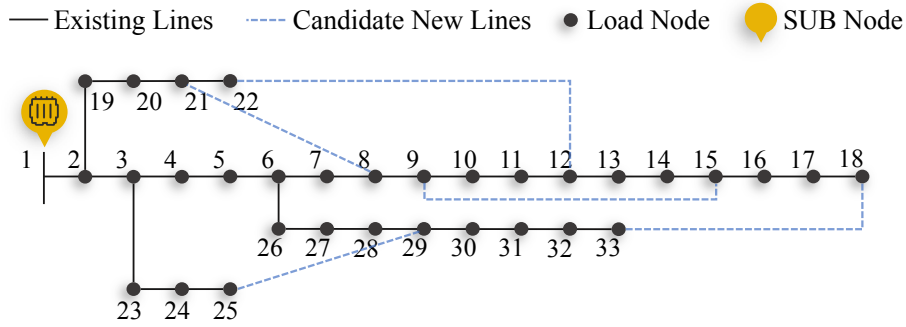

Figure 3.2   A modified 33-bus distribution system.

In terms of facility investment, we consider lines with three options varying in impedance, power capacity, and unit cost, and relevant parameters are aligned with Zhao et al.[79]. ESSs are considered to be built at the rest 32 nodes except the first one (slack bus), which is the substation node. Options of these facilities in the distribution system are given in Table 3.1. Besides, data sets for LMP named as $W_{\alpha,t}^{\text{LMP}}$ in Eq. (3.3) and the regulation price named as $W_{\text{REG},\alpha,t}^{\text{up}}/W_{\text{REG},\alpha,t}^{\text{dn}}$ in Eq. (3.4) can be consulted here[80].

Table 3.1   Options for the substation and ESSs in the distribution system.

Facilities	Different Options			
	Candidate nodes	Capacity (MVA/MWh)	Power (MW)	Construction cost (10^4US$)
		10	-	40
SUB	1	15	-	70
		20	-	110
		2	0.8	30
ESS	2-33	3.5	1.4	50
		5	2	90

3.7.2 Network Topology
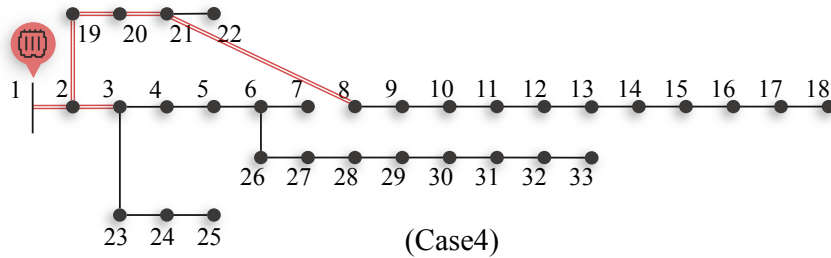
Figure 3.3   Final topology of the deterministic MILP in four cases.

Assuming that the planning scheme will last for 14 years, four cases are designed with the framework of the deterministic MILP proposed in Section 3.2 as below:

- Case 1: both regulation service revenue and degradation penalty of ESSs are included in the objective;
- Case 2: ESS degradation penalty is omitted;
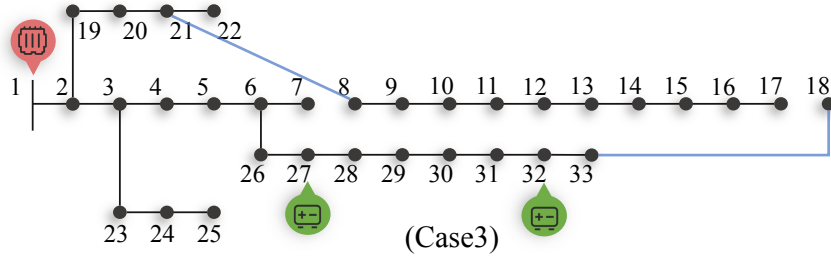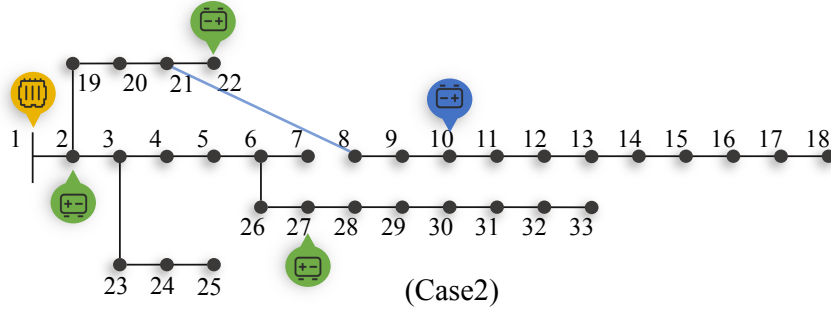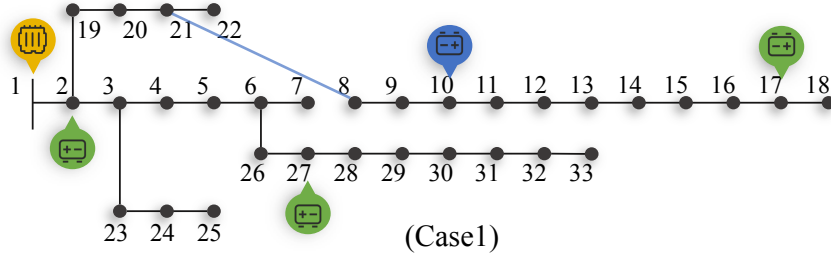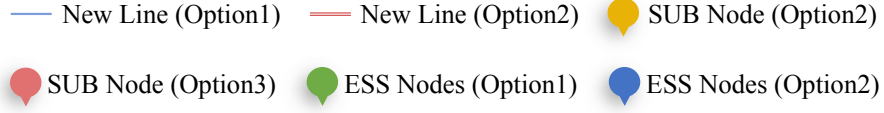- Case 3: regulation services of ESSs are ignored;
- Case 4: no ESS is built in the distribution system.

The network topology of four cases is shown in Fig. 3.3, where the capacity of Option1<Option2<Option3 for different facilities. For line construction, Case 1 and Case 2 both upgrade one feeder while the number for Case 3 and Case 4 is 2 and 6 respectively. The substation, meanwhile, expands to the highest capacity in Case 3 and Case 4. From the view of ESS deployment, the former two cases build more ESSs with larger capacities than that of the latter two.

These differences demonstrate that without enough storage units, peak shaving in the distribution system will be severely weakened, thus leading to the inevitability of feeder upgrades. Besides, ESSs can discharge to satisfy the increasing load demand and lower the requirements of substation capacity. Apart from Case 4 which does not consider ESSs, fewer ESSs are constructed in Case 3, which indicates that the revenue from regulation services is crucial to the economy of ESS investment.

3.7.3 Comparison of ESS Degradation

To further study the influence of degradation penalty in the objective function, normalization degradation curves of three cases with ESSs are compared in Fig. 3.4.
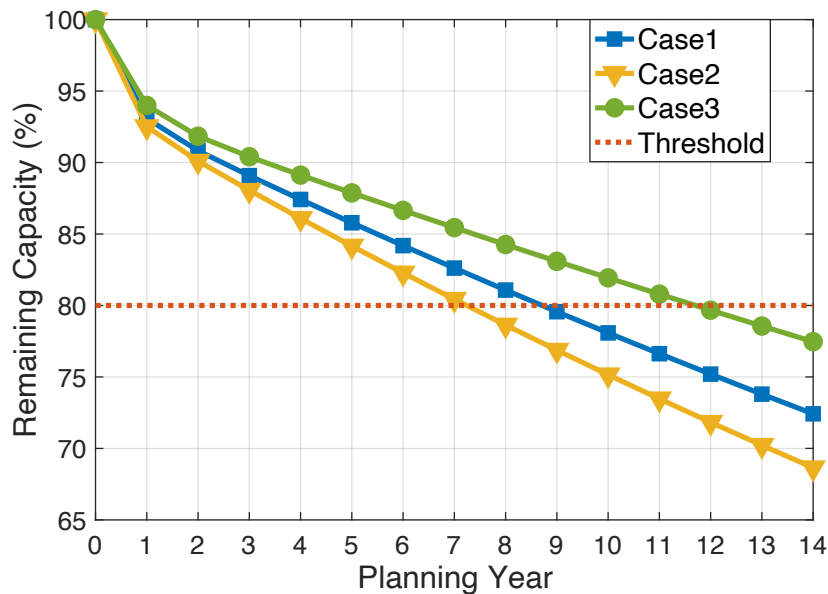

Figure 3.4   Capacity degradation behaviors of ESSs in Case 1-3.

In practice, the threshold of ESS remaining capacity for the distribution system operator (DSO) to end its use is set as 80% of the nominal value[18], such that ESSs in Case 2 only work for 7 years before retiring, while the periods for Case 1 and Case 3 are 8 and 11 years, respectively, hence the degradation penalty can prolong ESS lifetime for one year.

On the other hand, without providing regulation services, ESSs tend to have a longer lifespan as the curve of Case 3. Though ESS regulation capacity is much less than that of energy arbitrage, frequent regulation up and down in micro cycles are more harmful to the cell capacity than relatively slow and macro charge-discharge cycles.

To better observe the aging process, ESS's behaviors and its SOC in a typical day of Case 1 are illustrated as Fig. 3.5. Generally, the number of full charge-discharge cycles is about once per day, which adds up to 3000 to 4000 times in its 8-year lifespan. Besides, by comparing the LMP and charge/discharge bars, the energy arbitrage of ESSs which leverages the electricity price difference between peak and valley load hours is demonstrated.
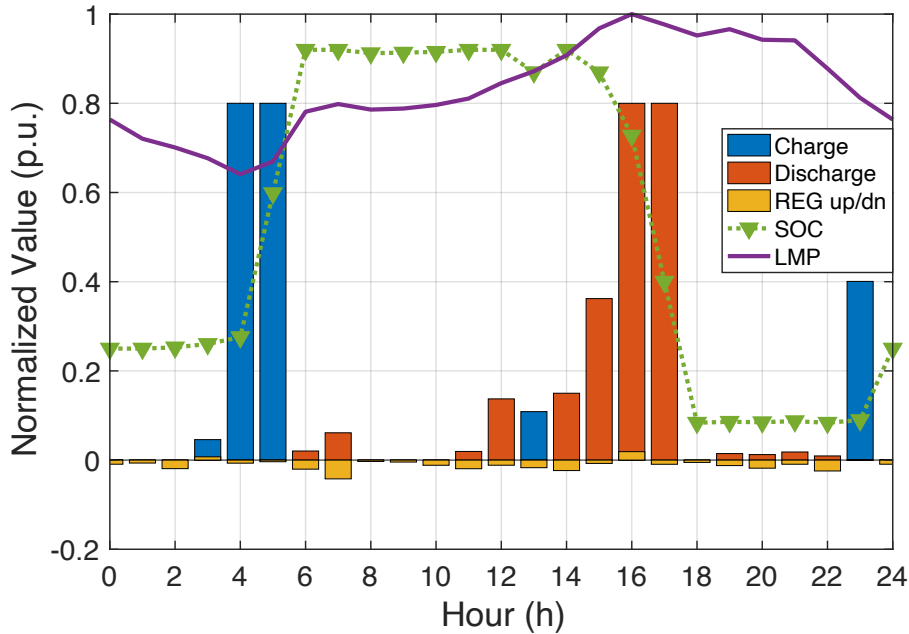
Figure 3.5   Relationship between ESS behaviors and the LMP in Case 1.

3.7.4 Economic Analysis

In Table 3.2, all discounted expenses constituting the overall planning cost are listed. Case 1 is the cheapest, while Case 4 is the most expensive one without ESS being built. The second-highest expense is that of Case 3, because no extra revenue can be earned from regulation services, which is crucial to ESS's profitability in a distribution system. And Case 2 being less economical than Case 1 is due to ESSs' early retirement.

Table 3.2   Discounted planning costs in four cases.

Terms (10^4US$)	Case 1	Case 2	Case 3	Case 4
Regulation service	✓	✓	✕	✕
ESS degradation	✓	✕	✓	✕
Total cost	527.14	527.52	535.37	618.37
Line investment	19.80	19.80	39.61	158.43
SUB investment	39.61	39.61	62.24	62.24
ESS investment	79.21	79.21	33.95	**0**
Total maintenance cost	17.11	16.71	18.03	15.53
Power transaction cost	380.51	380.71	381.18	382.18
Regulation revenue	9.74	8.52	**0**	**0**
Degradation penalty	0.63	**0**	0.37	**0**

Considering low ESS profitability in Case 3, higher fare on the substation and feeders is spent, because the limited capacity of ESS can not shave the peak load effectively. In Case 1 and Case 2, the ESS investment cost is the same. In other words, once regulation services are considered in the DSEP, the valuation of ESSs is improved significantly. Since Case 2 retires ESSs one year in advance, its total maintenance cost will be reduced. The highest maintenance cost is spent in Case 3, for it invests feeders and the substation with higher capacity. Subsequently, the least cost on purchasing electricity is found in Case 1 since its ESSs can carry out energy arbitrage one year longer than Case 2 and have a higher capacity than Case 3. Additionally, the early disposal of ESSs in Case 2 earns less regulation revenue due to the radical charge and discharge behaviors.
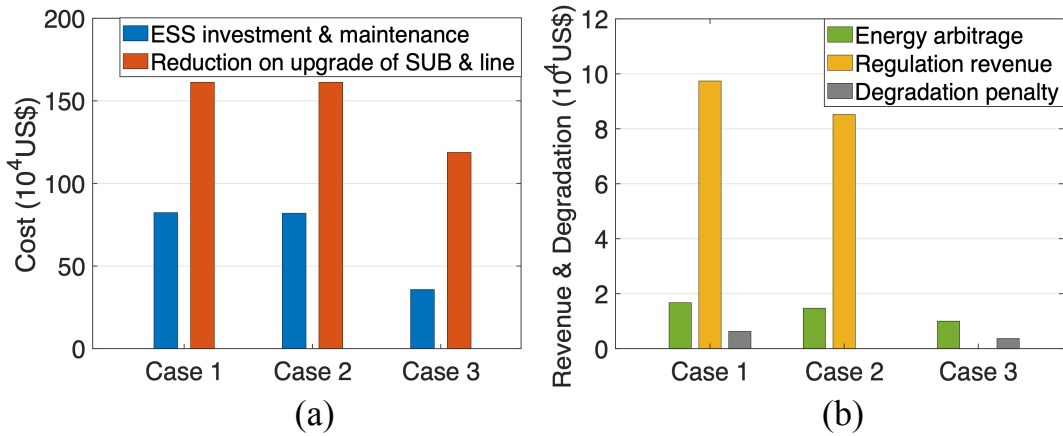

Figure 3.6   Profitability of ESSs in Case 1-3.

In Fig. 3.6, Case 1-3 are compared with Case 4 (No ESS), where their profits of en-

ergy arbitrage are calculated by differences in the power transaction cost shown in Table
3.2. It is observed from (a) that the investment and maintenance cost of ESSs is always
less than their reduction on the upgrade cost of the substation and lines, proving the econ-
omy of investing in ESSs in these cases. In (b), Case 1 with the highest degradation cost
also has the highest regulation revenue for a longer storage lifespan. Comparing to en-
ergy arbitrage, ESSs' providing frequency regulation services earns more money in the
distribution system. This normally happens when the regulation price dominates over the
LMP or the LMP has a relatively smooth peak and valley.

3.8 Conclusions

In this chapter, both regulation services and ESS degradation were considered in the
DSEP. We leveraged a MILP model on a 33-node distribution system to obtain the optimal
planning decisions of line configuration, substation expansion, and ESS siting and sizing.

In order to demonstrate the effect of ancillary service provision and battery degrada-
tion on ESS profitability, four cases were designed. By comparing their planning results,
we came to a conclusion that in a long enough planning period, the ESS revenue from
energy arbitrage and regulation services will exceed its investment and maintenance fee,
proving the economy of investing in this facility. Furthermore, with consideration of the
degradation term, ESS tends to have a longer lifespan thus ends up yielding higher rev-
enue. The profitability from regulation services and energy arbitrage was also compared,
in which ESS regulation up/down tends to be more harmful to its capacity but making
more money in unit time.

Regarding the ESS aging process, we also illustrated the ESS's cycle behavior in a
typical day of the optimal planning case. The general charge-discharge cycles add up
to 3000 to 4000 times in its 8-year lifetime, which is realistic and economically sound.
Through the comparison of the hourly LMP and charge/discharge power, ESS participat-
ing in energy arbitrage can be recognized in a legible manner.

CHAPTER 4 TWO-STAGE STOCHASTIC PROGRAMMING APPROACH

4.1 Overview

On the bedrock of the model formulation in Chapter 3, we propose to further incorporate uncertain factors, e.g., changing electricity prices and load demand, into DSEP in this chapter. Uncertainty is one of the most crucial characteristics of real power systems. And, uncertainty-based programming, in other words, stochastic programming often leads to different planning results from deterministic programming. Taking numerous uncertain parameters of planning problems is particularly challenging, which renders the appropriate scenario generation and efficient optimization extremely vital when confronting stochastic programming problems.

In this chapter, we treat the above-mentioned problem as two-stage stochastic programming. Multiple uncertainties are involved in the distribution system planning, including renewable power output, load demands, and electricity prices. To obtain representative scenarios, GMM is adopted to characterize historical data, then we are able to generate an infinite number of scenarios based on the learned GMM. To accelerate the solution of this stochastic linear program, the PH algorithm with parallel computing is developed, accompanied by an adjustable penalty factor to boost its convergence. At last, we demonstrate the effectiveness of both the planning model and the modified algorithm through numerical experiments.

4.2 Model Formulation

To address the uncertainty issue of load demand and electricity prices in DSEP, we further develop the deterministic MILP model as a two-stage stochastic program. In the first stage, optimal expansion decisions of the master problem are obtained, then in the second stage, the subproblem is solved to minimize the expected operation cost under previous investments. For each of the typical scenarios considered, the continuous solution of the second-stage economic operation is incorporated into the master problem for better planning decisions. When the difference between two adjacent iterations of the binary

decision variables becomes negligible, the final optimal expansion planning scheme is attained.

To reduce excessive variables as the number of scenarios increases, we assume that in the following context all facilities should go into operation once being built, which means the binary operating variable y equals the planning decision x. For convenience, we use x to represent all these investment/operating decisions on lines, substations, and ESSs.

4.2.1 Master Problem: First-Stage Expansion Planning

We assume that the substations, ESSs, and feeders are invested, owned, and operated by the DSO. The first-stage objective function (4.1) aims to minimize the overall cost spent during the planning stage, which can be divided into two groups: 1) the investment cost C_{INV} and maintenance cost C_{MAT} for distribution facilities. 2) the mathematical expectation of the operation cost in multiple scenarios, denoted by the recourse function $Q(x, y_s)$. The variable y_s which is continuous herein represents the optimal value of all decision variables in the second stage.

$$\min \sum_i \gamma^i \left(C_{\text{INV}} + C_{\text{MAT}} + \sum_{s=1}^{S} \theta_s Q(x, y_s) \right) \tag{4.1}$$

$$\sum_{j \in \Psi_{\text{eL}}} x_j^{\text{eL}} + \sum_{k \in \Psi_{\text{nL}}} \sum_z x_{k,z}^{\text{nL}} = \Gamma - N_{\text{SUB}} \tag{4.2}$$

$$\sum_b x_{m,b}^{\text{SUB}} \leq 1, \quad \forall m \in \Omega_{\text{SUB}} \tag{4.3}$$

$$\sum_e x_{n,e}^{\text{ESS}} \leq 1, \quad \forall n \in \Omega_{\text{ESS}} \tag{4.4}$$

$$x_j^{\text{eL}}, x_{k,z}^{\text{nL}}, x_{m,b}^{\text{SUB}}, x_{n,e}^{\text{ESS}} \in \{0, 1\}$$

$$\forall j \in \Psi_{\text{eL}}, k \in \Psi_{\text{nL}}, m \in \Omega_{\text{SUB}}, n \in \Omega_{\text{ESS}} \tag{4.5}$$

Eqs. (4.2)-(4.5) are constraints for the master problem, which have been explained in Section 3.5. Besides, as indicated in Eq. (4.5), all the first-stage decision variables of the MILP model are binary.

4.2.2 Subproblems: Second-Stage Operational Strategies

After a solution is obtained in the master problem, a subproblem can be solved where all decision variables are continuous. In the recourse function (4.6), we add the power transaction cost $W_{s,t}^{\text{LMP}} p_{m,b,s,t}^{\text{SUB}}$, the penalty due to unserved loads $M_{\text{cur}} d_{l,s,t}^{\text{cur}}$ and the battery degradation term $M_{\text{deg},t} \varphi_s^T \beta_{n,s,t}^{\text{ESS}}$, then minus the revenue earned by ESSs' selling regulation services $\left(W_{\text{REG},s,t}^{\text{up}} r_{n,s,t}^{\text{up}} + W_{\text{REG},s,t}^{\text{dn}} r_{n,s,t}^{\text{dn}} \right)$, where M_{cur} is a large number to avoid load curtailment. Compared with model formulation in Section 3.2, the subscript s is added to denote that the operation decision variables in $Q(x, y_s)$ are different among scenarios. It is necessary to determine the operation state of feeders, substations and ESSs in each scenario s.

$$
\begin{aligned}
Q(x, y_s) = \min \sum_{t=1}^{T} & \left(\sum_{m \in \Omega_{\text{SUB}}} W_{s,t}^{\text{LMP}} p_{m,b,s,t}^{\text{SUB}} + \sum_{l \in \Omega_D} M_{\text{cur}} d_{l,s,t}^{\text{cur}} \right. \\
& \left. + \sum_{n \in \Omega_{\text{ESS}}} M_{\text{deg},t} \varphi_s^T \beta_{n,s,t}^{\text{ESS}} - \sum_{n \in \Omega_{\text{ESS}}} \left(W_{\text{REG},s,t}^{\text{up}} r_{n,s,t}^{\text{up}} + W_{\text{REG},s,t}^{\text{dn}} r_{n,s,t}^{\text{dn}} \right) \right)
\end{aligned}
\tag{4.6}
$$

$$
\begin{aligned}
\Xi^{\text{eL}} f_{s,t}^{\text{eL}} &+ \Xi^{\text{nL}} f_{s,t}^{\text{nL}} + \sum_{l \in \Omega_D} d_{l,s,t}^{\text{cur}} + \sum_{m \in \Omega_{\text{SUB}}} p_{m,b,s,t}^{\text{SUB}} \\
&= \sum_{l \in \Omega_D} D_{l,s,t} - \sum_{n \in \Omega_{\text{ESS}}} \left(p_{n,s,t}^{\text{dis}} - p_{n,s,t}^{\text{ch}} + \omega_{s,t}^{\text{up}} r_{n,s,t}^{\text{up}} - \omega_{s,t}^{\text{dn}} r_{n,s,t}^{\text{dn}} \right) \cdot (1hr.)
\end{aligned}
\tag{4.7}
$$

$$
\left| Z_j^{\text{eL}} f_{j,s,t}^{\text{eL}} + [\Xi^{\text{eL}}]_{Rowj}^T u_{s,t} \right| \leq M \cdot (1 - x_j^{\text{eL}}) \quad \forall j \in \Psi_{\text{eL}}
\tag{4.8}
$$

$$
\left| Z_{k,z}^{\text{nL}} f_{k,s,t}^{\text{nL}} + [\Xi^{\text{nL}}]_{Rowk}^T u_{s,t} \right| \leq M \cdot (1 - x_{k,z}^{\text{nL}}) \quad \forall k \in \Psi_{\text{nL}}
\tag{4.9}
$$

$$
0 \leq d_{l,s,t}^{\text{cur}} \leq D_{l,s,t} \quad \forall l \in \Omega_D
\tag{4.10}
$$

$$
0 \leq p_{m,b,s,t}^{\text{SUB}} \leq \sum_b x_{m,b}^{\text{SUB}} E_{b,\max}^{\text{SUB}} \quad \forall m \in \Omega_{\text{SUB}}
\tag{4.11}
$$

$$
|f_{j,s,t}^{\text{eL}}| \leq x_j^{\text{eL}} F_{j,\max}^{\text{eL}}, |f_{k,s,t}^{\text{nL}}| \leq \sum_z x_{k,z}^{\text{nL}} F_{k,z,\max}^{\text{nL}} \quad \forall j \in \Psi_{\text{eL}}, \forall k \in \Psi_{\text{nL}}
\tag{4.12}
$$

$$\xi_{n,s,t+1}^{\text{SOC}} = \xi_{n,s,t}^{\text{SOC}} - (p_{n,s,t}^{\text{dis}} - p_{n,s,t}^{\text{ch}} + \omega_{s,t}^{\text{up}} r_{n,s,t}^{\text{up}} - \omega_{s,t}^{\text{dn}} r_{n,s,t}^{\text{dn}}) \cdot (1hr.)$$
$$\forall n \in \Omega_{\text{ESS}}, t = 1, 2, \cdots, 23 \tag{4.13}$$

$$0 \le \xi_{n,s,t}^{\text{SOC}} \le \sum_e x_{n,e}^{\text{ESS}} E_{e,\max}^{\text{ESS}} \tag{4.14}$$

$$(r_{n,s,t}^{\text{dn}} + p_{n,s,t}^{\text{ch}}) \cdot (1hr.) \le \sum_e x_{n,e}^{\text{ESS}} E_{e,\max}^{\text{ESS}} - \xi_{n,s,t}^{\text{SOC}} \tag{4.15}$$

$$(r_{n,s,t}^{\text{up}} + p_{n,s,t}^{\text{dis}}) \cdot (1hr.) \le \xi_{n,s,t}^{\text{SOC}} \tag{4.16}$$

$$\omega_{s,t}^{\text{up}} r_{n,s,t}^{\text{up}} + p_{n,s,t}^{\text{dis}} - \omega_{s,t}^{\text{dn}} r_{n,s,t}^{\text{dn}} \le \sum_e x_{n,e}^{\text{ESS}} P_{e,\max}^{\text{ESS}} \tag{4.17}$$

$$\omega_{s,t}^{\text{dn}} r_{n,s,t}^{\text{dn}} + p_{n,s,t}^{\text{ch}} - \omega_{s,t}^{\text{up}} r_{n,s,t}^{\text{up}} \le \sum_e x_{n,e}^{\text{ESS}} P_{e,\max}^{\text{ESS}} \tag{4.18}$$

$$r_{n,s,t}^{\text{up}} + p_{n,s,t}^{\text{dis}} \le \sum_e x_{n,e}^{\text{ESS}} P_{e,\max}^{\text{ESS}} \tag{4.19}$$

$$r_{n,s,t}^{\text{dn}} + p_{n,s,t}^{\text{ch}} \le \sum_e x_{n,e}^{\text{ESS}} P_{e,\max}^{\text{ESS}} \tag{4.20}$$

$$\xi_{n,s,t}^{\text{SOC}} = \sum_e x_{n,e}^{\text{ESS}} E_{e,0}^{\text{ESS}}, \quad t = 1, 24 \tag{4.21}$$

$$p_{n,s,t}^{\text{ch}}, p_{n,s,t}^{\text{dis}}, r_{n,s,t}^{\text{up}}, r_{n,s,t}^{\text{dn}} \ge 0 \tag{4.22}$$

There are two groups of the second-stage constraints: Eqs. (4.7)-(4.12) are for distribution system operation, and Eqs. (4.13)-(4.22) are for ESS operation. In the first group, we adopt a distribution system power flow model with DC-approximated voltage deviation by introducing KCL in (4.7), and node voltage limit in (4.8), (4.9). Constraints (4.10)-(4.12) impose limits on maximal load curtailment, substation's capacity and feeder's capacity, respectively.

By partitioning the battery's capacity into two parts, ESSs can achieve energy arbitrage by charging and discharging, while selling ancillary services by providing the regulation capacity. Eqs. (4.13)-(4.20) are physical constraints aligned with the settings of Foggo et al.[9]. Eq. (4.21) forces all ESSs to maintain the same SOC at the beginning and the end hour in a daily scene. The last constraint (4.22) pertains to the non-negativity of ESS decision variables. It is noteworthy that a Big-M method is also adopted as Eqs. (3.27)-(3.31), which is omitted in this section.

4.3 Solution Method

4.3.1 Modeling of Uncertainties

MCS based on single normal distribution may not well describe the diversity in power output, load demand, relevant prices, and policies, hence generate scenarios that result in deviation of the optimal solution from the actual economic scheme. In this work, a GMM is introduced with the assumption that the original data follow a linear superposition of K normal distributions[81] instead of a single one. Specifically, we suppose that scenarios are drawn from a joint distribution $P(X|Y)$ where the y_i is a random variable indicating from which normal distribution this scenario x_i is drawn. Therefore, the learning of GMM parameters $\hat{\mu}_k$ and $\hat{\sigma}_k$ lies in the maximal likelihood estimate scheme:

$$\{\hat{\mu}_k, \hat{\sigma}_k\}_1^K = \arg\min \prod_{i=1}^{n} P(x_i|y_i) \cdot P(y_i) \quad y_i \in \{1, \cdots, K\} \tag{4.23}$$

which is tractable through the expectation-maximization algorithm. A scenario is sampled from one of the K normal distributions as:

$$N(\mu_k, \sigma_k) \quad \text{for } k = 1, \cdots, K \tag{4.24}$$

In this work, we set $K = 4$ and for each K generate scenarios according to the weights of different normal distributions. For a given S and K, this sampling process can be described as:

$$\{x_i|y_i = k\}_{i=1}^{S \cdot P(y_i=k)} \sim N(\mu_k, \sigma_k) \quad \text{for } k = 1, \cdots, K \tag{4.25}$$

hence, we obtain S scenarios from these distributions. Fig. 4.1 illustrates the whole

procedure, where scenario x_i is a continuous vector, and the GMM is a weighted sum of four Gaussian distributions, with the corresponding weights $P(y_i = 1)$, $P(y_i = 2)$, $P(y_i = 3)$, $P(y_i = 4)$, respectively. Based on the well-estimated parameters of the GMM, we can easily generate adequate scenarios via the MCS method.
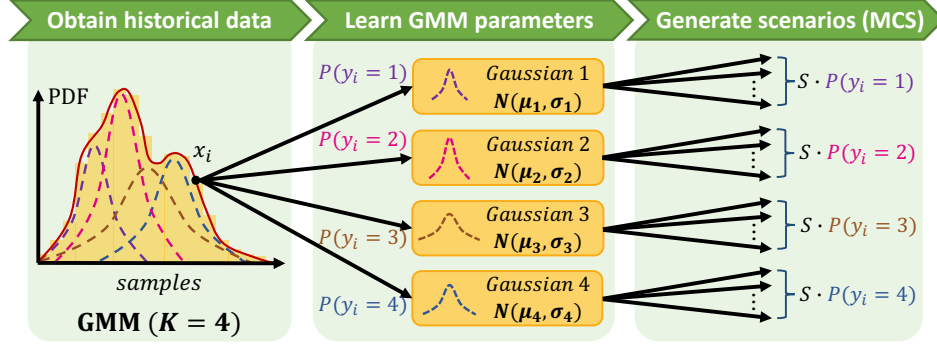

Figure 4.1   Procedure of uncertainty modeling (PDF: the probability density function; MCS: the Monto Carlo simulation method based on GMM).

4.3.2 L-Shaped Method

The L-shaped method is named for its dual block-angular structure[48], where the simplex multiplies need to be calculated in adding feasibility cuts and optimality cuts, which are two major steps (Step 2 and Step 3) in Fig. 4.2 .

A linear program presented in Eq. (4.26) named master problem is solved in Step 1, whose decision variables are the first-stage binary ones x_j^{eL}, $x_{k,z}^{\mathrm{nL}}$, $x_{m,b}^{\mathrm{SUB}}$, $x_{n,e}^{\mathrm{ESS}}$ and the lower bound ϕ of the second-stage recourse. Once the optimal solution (x^v, ϕ^v) is obtained, we come to Step 2 to check the feasibility of the subproblem. Note that for the first loop $v = 1$, ϕ is ignored with its initial value ϕ^v set as $-\infty$, and both the F_{cut}^r and O_{cut}^u representing the feasibility and optimality cuts are empty.

$$\min \mathbb{Z} = \sum_i \gamma^i \left(C_{\mathrm{INV}} + C_{\mathrm{MAT}} + \phi \right)$$

(4.26)

s.t. Constraints (4.2)-(4.5) & F_{cut}^r & O_{cut}^u.

In Step 2, variable v_a is utilized to detect any violation in all subproblem constraints (4.7)-(4.22) & (3.27)-(3.31), we move all their terms to the left side of the sign and leave v_a at right, then the modified constraints mentioned in (4.27) are obtained $\left(\text{i.e. Eq. (4.16)}\right.$ is reformulated as $(r_{n,s,t}^{\mathrm{up}} + p_{n,s,t}^{\mathrm{dis}}) \cdot (1hr.) - \xi_{n,s,t}^{\mathrm{SOC}} \le v_a \Big)$. After eliminating non-negative restrictions like (4.22), the number of subproblem constraints SC numerically equals v_a.
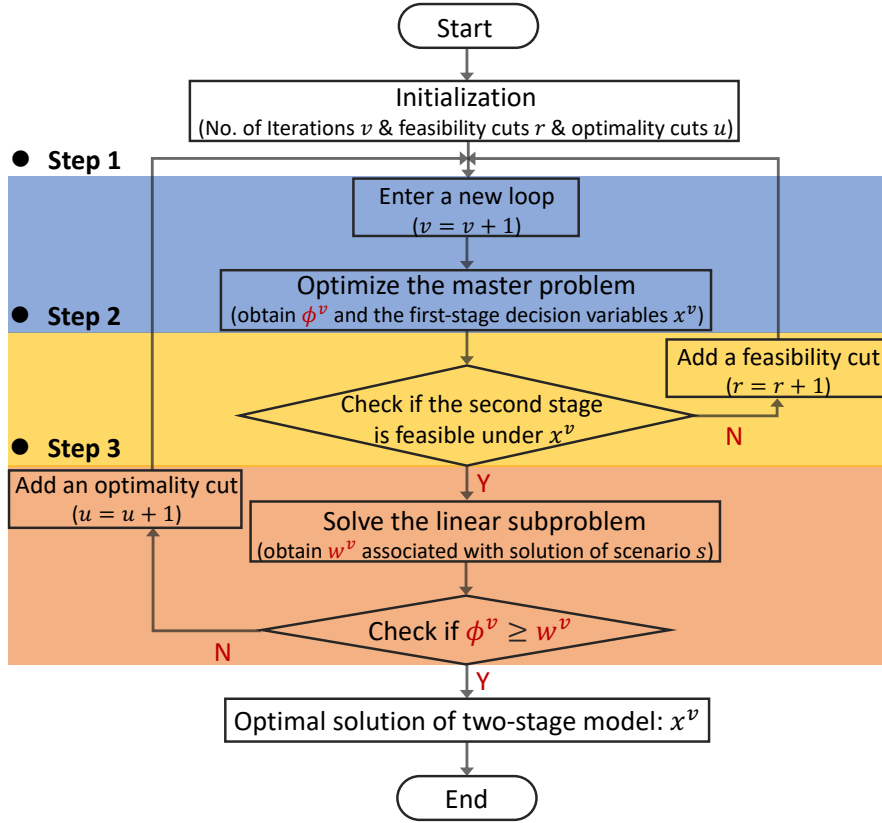
Figure 4.2   Flow chart of the L-shaped method.

$$\min \mathbb{W}'_s = \sum_{a \in SC} |v_a| \tag{4.27}$$

s.t. Modified Constraints (4.7)-(4.22) & (3.27)-(3.31).

The absolute values of all v_a elements are added up as $\mathbb{W}'_s$ in Eq. (4.27), which is minimized under all scenarios and compared with 0. If any $\mathbb{W}'_s$ is larger than the tolerance threshold 1e-5, then Step 1 needs to be recalculated with one feasible cut $(\tau^v)^T(T_s x - h_s) \geq 0$ added to F^r_{cut}. Here τ^v defines the associated simplex multipliers with the optimal solution of (4.27). T_s and h_s denote the coefficient of x and the constant in Eqs. (4.7)-(4.22) & (3.27)-(3.31) under scenario s, respectively.

$$\min \mathbb{W}_s = Q(x, y_s) \tag{4.28}$$

s.t. Constraints (4.7)-(4.22) & (3.27)-(3.31).

When all $\mathbb{W}'_s$ equal 0, (x^v, ϕ^v) obtained in Step 1 is demonstrated feasible for the second-stage problem, then the algorithm will proceed with Step 3. The second-stage expense $\mathbb{W}_s$, which equals $Q(x, y_s)$ in (4.6), is solved in Eq. (4.28) and the constraints are

original formulations of (4.7)-(4.22) & (3.27)-(3.31) this time. The optimal w^v is derived from $w^v = \sum_{s=1}^{S} \theta_s (\pi_s^v)^T (h_s - T_s x^v)$, where π_s^v is the simplex multipliers of the solution in (4.28) under each scenario. Subsequently, $\phi^v \leq w^v$ is checked, if it is satisfied, the algorithm will end with the optimal investment decision x^v. Conversely, Step 1 will be recalculated with one optimal cut $\sum_{s=1}^{S} \theta_s (\pi_s^v)^T (h_s - T_s x) \leq \phi$ added to O_{cut}^u.

In this work, considering that Eq. (4.27) in Step 2 and (4.28) in Step 3 are solved in each scenario, Parallel Computing Toolbox™ with MATLAB interface is adopted for accelerating optimization by *parfor*-loops in multiple threads. Theoretically, if there are enough workers available, the optimization can be solved concurrently with one scenario in a single thread.

Algorithm 3: L-shaped Method with Parallel Computing.

---

1. **Input:** all parameters in the **Nomenclature**.
2. **Initialization:** $r = u = v = 0$.
3. **while** $\phi^v < w^v$ **do:** $v \leftarrow v + 1$.
4.   **if** $u = 0$ **solve:** (4.26) for x^v.
5.   **else solve:** (4.26) for (x^v, ϕ^v).
6.   **end if**
7.   Set: $F = 1$.
8.   **parfor** $s \in S$ **solve:** (4.27) for $\mathbb{W}_s'$.
9.   **end parfor**
10.   **for** $s \in S$
11.   **if** $\mathbb{W}_s' \geq 10^{-5}$ **do:** $F \leftarrow 0$ **break**.
12.   **end if**
13.   **end for**
14.   **if** $F = 0$ **do:**$r \leftarrow r + 1$, $F_{cut}^r = \left[F_{cut}^r, (\tau^v)^T (T_s x - h_s) \geq 0 \right]$.
15.   **end if**
16.   **if** $F = 1$
17.   **parfor** $s \in S$ **solve:** (4.28) for $\mathbb{W}_s$.
18.   **end parfor**
19.   Update: $u \leftarrow u + 1$, $w^v = \sum_{s=1}^{S} \theta_s (\pi_s^v)^T (h_s - T_s x^v)$.
20.   **do:** $O_{cut}^u = \left[O_{cut}^u, \sum_{s=1}^{S} \theta_s (\pi_s^v)^T (h_s - T_s x) \leq \phi \right]$.
21.   **end if**
22. **end while**

In the pseudo-code applied for our two-stage MILP model, F is the flag for subproblem's feasibility. Considering that **break** should not exist in *parfor*-loops, steps 10-13 has been separated from 8-9. The corresponding serial number for Step 1, Step 2 and Step 3 is 3-6, 7-15 and 16-21, respectively. Obviously, the complexity of Step 2 determines the efficiency of the L-shaped method to a great degree.

Differing from some economic dispatch models where Step 2 is simply omitted,

for a DSEP problem, however, the first-stage expansion decisions can not guarantee the second-stage operation being always feasible. In fact, without adding feasibility cuts in the planning model, the optimal solution in most cases is to build as few distribution facilities as possible, which may conflict with the limits on the maximal capacity of current facilities, such as feeders and substations. In some sense, DSEP first searches for solutions that are feasible for the excessive load demand and then selects cost-optimal ones.

4.3.3 Progressive Hedging Algorithm

To simulate real conditions of distribution systems considering uncertainties in different seasons, days, and hours, numerous daily operation scenarios are randomly generated by the MCS method. However, the computation time will become intractable when too many scenarios are included. Hence, we adopt a decomposition technique to address the tractability issue and promote convergence. To determine a better option between the L-shaped method and the PH algorithm, we compare their basic rules and come to a conclusion.

As for the L-shaped method, the algorithm efficiency relies on iterations between the master problem and subproblem, i.e. the feasibility cuts and optimality cuts. It is effective for some specific models because the feasibility check of the subproblem can be omitted. Nevertheless, for a DSEP, the feasibility check of the first-stage planning results is unavoidable. Besides, considering the sitting and sizing of facilities like ESSs will add even more computational burden, which probably makes the L-shaped method less efficient in solving DSEP problems.

The significant feature of the PH algorithm, however, lies in the scenario-based decomposition technique. That is, for a large-scale MILP model with numerous scenarios, the PH algorithm can solve the subproblem in a paralleled way, thus improving the efficiency dramatically. Here, based on the PH algorithm proposed by Watson et al.[51], we decompose the two-stage stochastic model in Section 4.2 and apply PH to accelerate its convergence.

For notation simplicity, in the following context we define the set of planning decision variables as a new vector X_s in (4.29) and (4.30). A modified formulation of $\mathbb{Q}(s)$ in the subproblem of scenario s is denoted by (4.31).

$$X_s := \left\{ x_{j,s}^{\text{eL}}, x_{k,z,s}^{\text{nL}}, x_{m,b,s}^{\text{SUB}}, x_{n,e,s}^{\text{ESS}} \,\middle|\, \sum_b x_{m,b,s}^{\text{SUB}} \leq 1, \right.$$

$$\sum_e x_{n,e,s}^{\text{ESS}} \leq 1, \quad \sum_{j \in \Psi_{\text{eL}}} x_{j,s}^{\text{eL}} + \sum_{k \in \Psi_{\text{nL}}} \sum_z x_{k,z,s}^{\text{nL}} = \Gamma - N_{\text{SUB}}, \tag{4.29}$$

$$\left. x_{j,s}^{\text{eL}}, x_{k,z,s}^{\text{nL}}, x_{m,b,s}^{\text{SUB}}, x_{n,e,s}^{\text{ESS}} \in \{0, 1\} \right\}$$

$$X_s(q) = \begin{cases} x_{j,s}^{\text{eL}} & q = 1 \\[2mm] x_{k,z,s}^{\text{nL}} & q = 2 \\[2mm] x_{m,b,s}^{\text{SUB}} & q = 3 \\[2mm] x_{n,e,s}^{\text{ESS}} & q = 4 \end{cases} \tag{4.30}$$

$$\mathbb{Q}(s) = \min_{X_s, y_s} \sum_i \gamma^i \left(C_{\text{INV}} + C_{\text{MAT}} + \sum_{s=1}^S \theta_s Q(x, y_s) \right) \tag{4.31}$$

s.t. Constraints (4.7)-(4.22) & (3.27)-(3.31).

4.3.3.1 Computing Rational Vector $\bar{X}$

When making an investment plan, the decision-maker may know nothing about which scenario will be realized in the future. To avoid decisions dependent on specific scenarios, the *non-anticipativity* constraints are introduced as Eq. (4.32).

$$\begin{cases} x_{j,s}^{\text{eL}} = \bar{x}_j^{\text{eL}} & \forall j \in \Psi_{\text{eL}} \\[2mm] x_{k,z,s}^{\text{nL}} = \bar{x}_{k,z}^{\text{nL}} & \forall k \in \Psi_{\text{nL}} \\[2mm] x_{m,b,s}^{\text{SUB}} = \bar{x}_{m,b}^{\text{SUB}} & \forall m \in \Omega_{\text{SUB}} \\[2mm] x_{n,e,s}^{\text{ESS}} = \bar{x}_{n,e}^{\text{ESS}} & \forall n \in \Omega_{\text{ESS}} \end{cases} \tag{4.32}$$

In PH algorithms, these constraints are implicitly implemented. After calculating the average solution $\bar{X}$ of the first-stage decision vector X_s over all scenarios, the deviation $\|X_s - \bar{X}\|$ will be punished in the objective to ensure that all planning decisions in $s \in S$ are prone to approaching a common $\bar{X}$ after finite iterations. In general, $\bar{X}$ is a mathematical expectation derived from $\sum_{s \in S} \theta_s \cdot X_s$, and will be affected by every X_s. However, in DSEP problems, especially those considering large uncertainties, chances are that overload happens in some rare cases where distribution facilities such as feeders,

substations, and ESSs with larger capacity are necessary. Given this circumstance, if we continue to average planning decision variables over all scenarios, it is more likely to see non-convergence or unacceptable long run-time in the PH algorithm, since $\bar{X}$ will tend to approach the solution with less investment but more frequent occurrence, leading to a large punishment on decision variables of overload scenarios. Nevertheless, the overload scenario has little chance to converge to the average solution, otherwise, the subproblem will become infeasible.

The solution to a DSEP problem is supposed to be feasible in all scenarios involved. Hence, we give higher priority to the overload scenarios, in other words, the most radical investment solutions and calculate their expectations as a rational vector $\bar{X}$ shown below:

$$
\bar{X}^v(q) = \begin{cases} \sum_{s \in S} \theta_s \cdot x_{j,s}^{v,\mathrm{eL}} & q = 1 \\ \sum_{s \in S_{\mathrm{nL}}} \theta_s \cdot x_{k,z,s}^{v,\mathrm{nL}} & q = 2 \\ \sum_{s \in S_{\mathrm{SUB}}} \theta_s \cdot x_{m,b,s}^{v,\mathrm{SUB}} & q = 3 \\ \sum_{s \in S_{\mathrm{ESS}}} \theta_s \cdot x_{n,e,s}^{v,\mathrm{ESS}} & q = 4 \end{cases}
\tag{4.33}
$$

where $\bar{X}^v(q)$ is the new average solution of decision variables in iteration v, and S_{nL}, S_{SUB}, S_{ESS} are scenario sets producing planning results with feeders, substations and ESSs of largest capacity, respectively. As for decision variables denoting existing lines' investment, the corresponding $\bar{X}$ is still the mathematical expectation of $x_{j,s}^{v,\mathrm{eL}}$ in all scenarios since the original feeders can not address extreme cases like overload effectively.

As a result, the algorithm converges to a rational solution faster, for the DSEP with more distribution facilities to built is always feasible in normal load scenarios. To avoid over-investment in this scheme, sometimes only the average solution of the most crucial and complex decision variables, i.e. ESS investment, will be handled as Eq. (4.33) does.

4.3.3.2 Parallel Computing Process

Since each subproblem is independently solved in PH algorithms, the optimization in one scenario does not rely on others. Parallel Computing Toolbox™ with MATLAB interface is adopted by *parfor*-loops in multiple threads.

Theoretically, if there are enough processors available, the optimization can be solved concurrently with one scenario in a single thread. Consequently, the parallel processing can be applied to the PH designed for Eq. (4.31) as illustrated in the **Algorithm 4**:

Algorithm 4: PH Algorithm with Parallel Computing.

---

1. **Input:** PH parameters ε, $\rho(q)=\{\rho_{\text{eL}}, \rho_{\text{nL}}, \rho_{\text{SUB}}, \rho_{\text{ESS}}\}$.
2. **Initialization:** $v \leftarrow 1, w_s^{v-1} \leftarrow 0, g^v \leftarrow 0, \forall s \in S$.
3. **parfor** $s \in S$ **do:**
4. $X_s^v \leftarrow \operatorname{argmin}_{X_s,y_s} \mathbb{Q}(s)$ s.t. (4.7)-(4.22) & (3.27)-(3.31).
5. **end parfor**
6. Update: $\bar{X}^v$ according to Eq. (4.33).
7. **for** $s \in S$ **do:** $w_s^v \leftarrow w_s^{v-1} + \sum \rho(q)(X_s^v - \bar{X}^v)$.
8. **end for**
9. Update: $g^v \leftarrow \sum_{s \in S} \theta_s \cdot \|X_s^v - \bar{X}^v\|$.
10. **while** $g^v \geq \varepsilon$ **do:** $v \leftarrow v + 1$.
11.   **parfor** $s \in S$ **do:**
12. $X_s^v \leftarrow \operatorname{argmin}_{X_s,y_s} \left(\mathbb{Q}(s) + w_s^{v-1} \cdot X_s + \frac{\sum \rho(q)}{2} \cdot \|X_s - \bar{X}^{v-1}\|^2 \right)$.
13.   **end parfor**
14.   **repeat Step 6-8**.
15.   Update: $g(q)^v=\{g_{\text{eL}}^v, g_{\text{nL}}^v, g_{\text{SUB}}^v, g_{\text{ESS}}^v\}$ in **Step 9**.
16.   **for** q=1:4
17.   **if** $0 < g(q)^v \leq 1$ **do:** $\rho(q) = \left(1 + A(q)g(q)^v\right) \cdot \rho(q)$.
18.   **else do:** $\rho(q) = \left(1 + B(q)(g(q)^v - 1)\right) \cdot \rho(q)$.
19.   **end if**
20.   **if** $g(q)^v \geq g(q)^{v-1}$ **do:** $\rho(q) = \left(2 + A(q)g(q)^v\right) \cdot \rho(q)$.
21.   **end if**
22.   **end for**
23. **end while**

4.3.3.3 Gap-Dependent Penalty Factor

Empirically, planning results are found sensitive to the penalty factors. While a large ρ can push to the early termination, it can also harm the economy of facilities to be invested, i.e. the optimality of final solutions. By contrast, a small ρ cannot effectively penalize the deviation of planning variables from their average solution $\bar{X}$. What is worse, for MILP models with binary planning decisions, sometimes the optimization falls into endless loops due to $g(q)^v$ in Step 15 of **Algorithm 4** becoming fixed after several PH iterations. In this case, a belated change of penalty factors can hardly address the situation since the oscillation of some integer variables has occurred, and thus lead to endless cycling.

To deal with it, we adopt gap-dependent $\rho(q)$ values for better convergence rates while ensuring the solution quality. In Step 16-22 of the pseudo-code, the gap values $g(q)^v$ of the line, substation, and ESS planning decisions are divided into two groups: for those smaller than 1, we perform Step 17 to increase their $\rho(q)$ values; for others larger than 1, Step 18 is conducted. $A(q)$ and $B(q)$ here represent vectors including the tuning parameters for ρ_{eL}^v,

ρ_{nL}^{v}, ρ_{SUB}^{v}, ρ_{ESS}^{v}, and can be adjusted for different models while their values are usually around 1.

Both in Step 17 or Step 18, all $\rho(q)$ values are increased to a relatively small extent, and the initial $\rho(q)$ should be consequently smaller than the magnitude of the unit cost (C and O) of different distribution facilities. For early iterations, the PH algorithm will yield large reductions in gaps, then Step 18 will be effective to punish the deviation of binary variables among different scenarios, by increasing the penalty factors with a degree depending on current gaps. Here, $B(q)$ is used to rescale the distance between $g(q)^{v}$ and 1 for faster convergence.

However, the majority of PH iterations actually act in narrowing the already tiny gaps which are usually smaller than 1. Then Step 17 comes into play, where we use $\left(1 + A(q)g(q)^{v}\right)$ as the coefficient of $\rho(q)$, to ensure the penalty factors' linearly increasing with the changing gap. Instead of $A(q)g(q)^{v}$, the coefficient in Step 17 guarantees the continuous growth of $\rho(q)$ values even if $g(q)^{v}$ becomes quite small. In this case, though, the increment of $\rho(q)$ may not promote a convergence efficiently. Hence, Step 20-21 act as a soft means of *slamming* compared with that of Watson et al.[51], to avoid a rising $g(q)^{v}$.

The rapid increase in penalty factors probably results in premature convergence of some decision variables due to excessive punishment in $\|X_{s}^{v} - \bar{X}^{v}\|$. As a result, $B(q)$ tends to be less than $A(q)$, since in early iterations the gaps are large and cause significant growth in the penalty factors of Step 18. In fact, a relatively small $\rho(q)$ can be adopted at first, then increased progressively, yielding less impact on solution quality while ensuring convergence.

4.4 Case Study

As for the two-stage stochastic model in Section 4.2, it is solved in 4, 20, 40 and 100 scenarios by two algorithms mentioned in Section 4.3.2 and 4.3.3. Considering uncertainties from load demand, LMP, regulation signals, and prices, we try to find a planning scheme of higher reliability and practicability.

4.4.1 Impact of Considering Uncertainties

In Fig. 4.3, the topologies of the two-stage stochastic MILP model in 4, 20, 40 and 100 scenarios are illustrated as (a), (b), (c) and (d). When considering more scenarios

involving a wilder range of uncertainties, the planning scheme tends to become conservative with more feeders built in (c) and (d), which may cope with some extreme cases of overload.
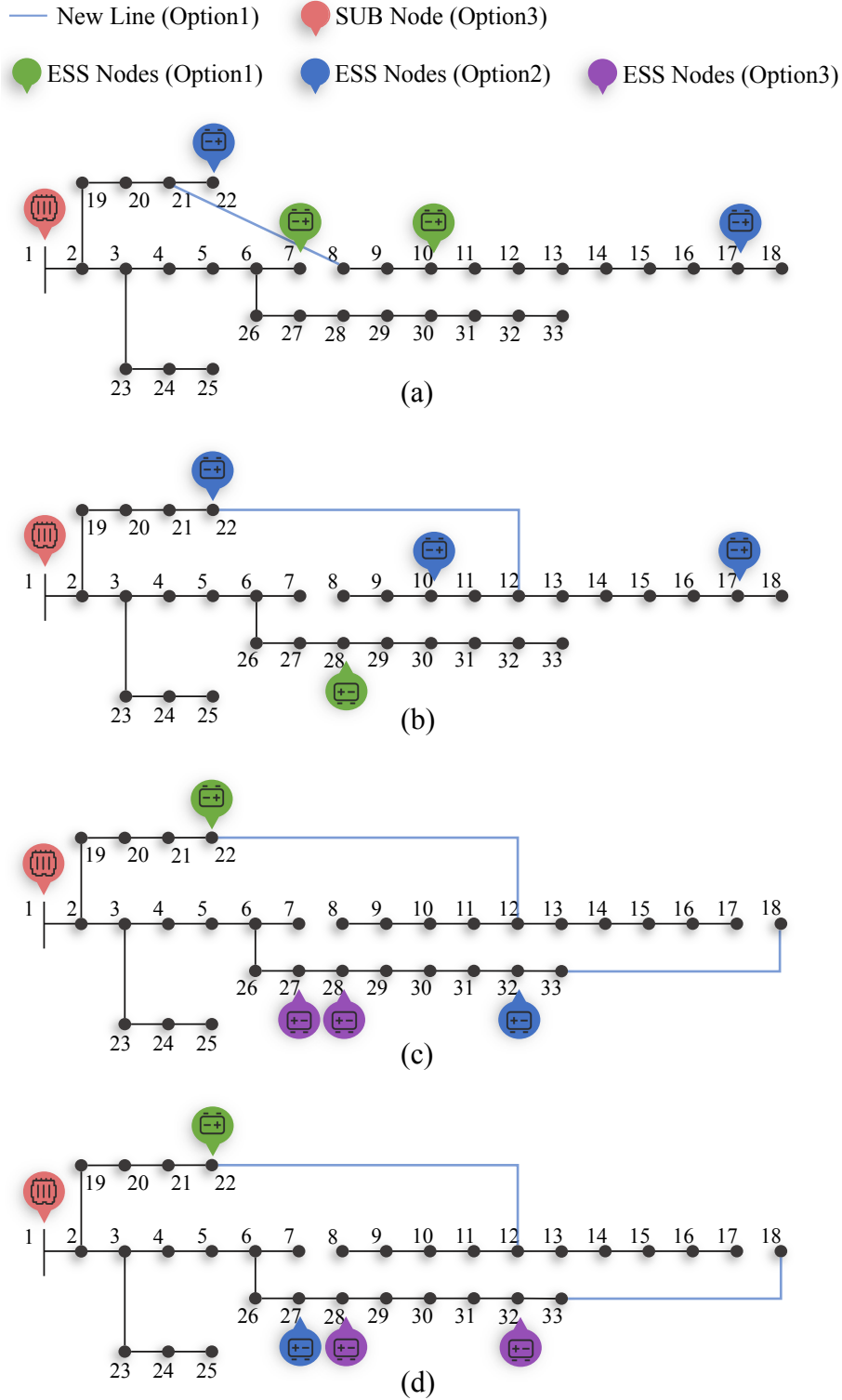

Figure 4.3   Network topology of the two-stage stochastic DSEP in scenario 4-100.

As illustrated in Table 4.1, planning results in different scenarios are listed and com-

pared with that of the deterministic MILP model. As the number of scenarios increases, the occurrence of overload or unusual regulation signals will be more likely. To ensure the load balancing all the time, more expensive feeders and ESSs need to be built. Consequently, the overall planning expense in 100 scenarios is more reliable in real conditions, however, not the most economical one.

Table 4.1   Comparison of planning results of the deterministic MILP and two-stage stochastic MILP.

DSEP Models	Deterministic	Two-stage stochastic MILP			
$(10^4$US$)$	MILP	S=4	S=20	S=40	S=100
Total cost	527.14	598.46	603.05	667.29	664.04
Line investment	19.80	19.80	19.80	39.61	39.61
SUB investment	39.61	62.24	62.24	62.24	62.24
ESS investment	79.21	90.53	101.85	147.11	147.11
Total maintenance cost	17.11	19.94	20.39	22.04	22.04
Power transaction cost	380.51	415.78	409.38	409.66	406.26
Regulation revenue	9.74	10.37	11.19	14.07	13.92
Degradation penalty	0.63	0.54	0.58	0.70	0.70

Moreover, a positive correlation between the total cost spent in DSEP and the scenarios considered does not exist. Actually, the highest expense is shown in the result of S=40 as 6.6729 million dollars, since fewer scenarios generated from normal distributions have higher randomness which may lead to a deviation from the optimal solution. With more scenarios included in S=100, the power transaction cost and regulation revenue reflecting ESS's participation in energy arbitrage and regulation services tend to be the closest to real expectation values among all the cases listed here.

4.4.2 Evaluation of Algorithm Performance

The performance of the L-shaped method and the modified PH algorithm is compared with the Gurobi 8.1.1 in Table 4.2. With a 2.40 GHz Intel Core i5 processor and 8 GB of memory, the speed of the modified PH is proved to be nearly 2-8 times of Gurobi optimizer, and 3-15 times of the L-shaped method. However, the superiority of the L-shaped method is revealed in its consistent approximation to the optimum solutions, while the modified PH is more heuristic as discussed before.

Frankly, chances are that time savings obtained by PH-based algorithms may come

Table 4.2　Comparison of computation time and solution quality among three solution methods in different scenarios.

Scenario	Method	Time (s)	Objective (10⁴US$)	Gap (%)
	Gurobi	46.213	598.46	0.0027
4	L-shaped Method	79.009	598.47	0.0048
	Modified PH	22.112	598.46	0.0023
	Gurobi	430.607	603.05	0.0122
20	L-shaped Method	672.774	603.05	0.0122
	Modified PH	141.251	603.05	0.0122
	Gurobi	2478.567	667.29	0.0109
40	L-shaped Method	2979.775	667.29	0.0109
	Modified PH	312.311	667.29	0.0107
	Gurobi	4501.718	664.04	0.0416
100	L-shaped Method	13916.344	664.04	0.0416
	Modified PH	872.529	672.69	1.3262

with a larger final optimality gap (S=100). Repeated experiments on more effective penalty factors are needed but even so the optimal ρ is not easy to find. Considering that, great research value lies in improving the solution quality of PH without harming its efficiency, with which we are trying to come up in Section 4.3.3. For DSEP with numerous decision variables, the PH algorithm can accelerate the convergence but not ensure the optimality of planning results.

Table 4.3　Tuning parameter values of the modified PH algorithm.

Scenario	Tuning parameters	
	A(q)	*B(q)*
4	1, 1, 1, 1	0.4, 0.4, 0.5, 0.8
20	1, 1, 1, 1.2	0.4, 0.4, 0.4, 0.3
40	1.2, 1.2, 1, 1	0.7, 0.8, 0.5, 0.5
100	1.2, 1.5, 1, 1	0.5, 0.8, 0.5, 0.4

For our model proposed in Section 4.2, tuning parameters of the modified PH are listed in Table 4.3. As mentioned in Section 4.3.3, we develop three algorithmic enhancements to the basic PH proposed by Watson et al.[51]. To prove their effectiveness, four

PH algorithms are defined and compared as follows:

- Basic PH: neither computes a rational average solution in Section 4.3.3.1 nor adopts gap-dependent penalty factors in Section 4.3.3.3;

- Average-solution PH: adopt the average solution to implement *non-anticipativity* constraints;

- Gap-dependent PH: adopt gap-dependent penalty factors and use the same tuning parameters as those in Table 4.3;

- Modified PH: adopt both algorithmic enhancements and is illustrated as the pseudo-code in Section 4.3.3.2.

Table 4.4   Comparison of computation time and solution quality among four kinds of PH algorithms in different scenarios.

Scenario	Method	Iteration	Time (s)	Gap (%)
4	Basic PH	17	85.481	0.0023
	Average-sol PH	7	34.913	3.4157
	Gap-dependent PH	5	27.389	0.0023
	Modified PH	4	22.112	0.0023
20	Basic PH	> 100	–	–
	Average-sol PH	15	454.266	0.0122
	Gap-dependent PH	13	432.274	0.0122
	Modified PH	6	141.251	0.0122
40	Basic PH	> 100	–	–
	Average-sol PH	70	6161.924	0.0107
	Gap-dependent PH	> 100	–	–
	Modified PH	5	312.311	0.0107
100	Basic PH	> 100	–	–
	Average-sol PH	9	1236.343	1.4447
	Gap-dependent PH	> 100	–	–
	Modified PH	5	872.529	1.3262

Considering that parallel computing technique has been widely used, we develop all the above algorithms with *parfor*-loops. Besides, they are started with the same initial values of penalty parameters ρ. In Table 4.4, the performance of four kinds of PH is compared and the superiority of the modified one is reflected in terms of computation

time and solution quality.

To save time, we set the maximal iteration as 100. In fact, the running time of one iteration is almost the same among four PH algorithms in a single scenario, for those failing to converge within 100 iterations, their computation time far exceeds others. It is noteworthy that both the modified PH and the average-solution PH can converge within 100 iterations in the case with 4-100 scenarios, while the gap-dependent PH converges in 4 and 20 scenarios. The use of a rational average solution, therefore, is proved to be more efficient in quickly achieving convergence than computing the mathematical expectation. By comparing the average-solution PH and gap-dependent PH with the basic one respectively, both algorithmic enhancements accelerate PH convergence by cutting down iterations to a certain degree. The modified PH converge with the lowest iteration time and optimality gap among these four algorithms, which further demonstrates the effectiveness of combining the above-mentioned algorithmic enhancements.
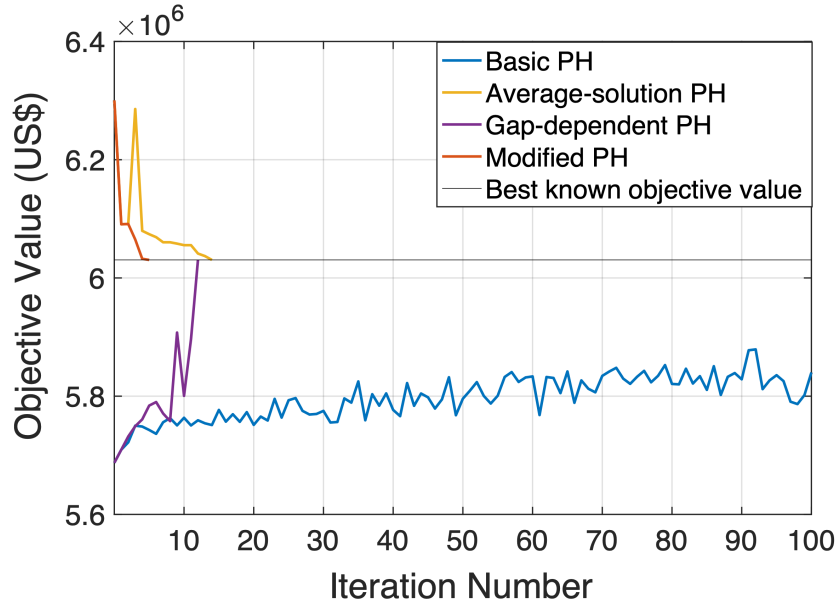

Figure 4.4   Objective values throughout iterations of four kinds of PH algorithms.

These four PH convergence profiles for the experiments performed in 20 scenarios are given in Fig. 4.4, in which we provide plots of iteration number versus objective values, to represent the total planning cost in each iteration. The modified PH and average-solution PH have decreasing trends of objective values before convergence, since they both adopt the average solution which reflects more distribution facilities invested to address overload cases. As illustrated in the plot, only basic PH tends to display cycling behaviors within 100 iterations. And the effective use of algorithmic enhancements in Section 4.3.3.1 and 4.3.3.3, both yield rapid iteration improvement in objective values of

the average-solution PH and gap-dependent one.

4.5 Conclusions

In this chapter, we reformulated the previous deterministic planning model to two-stage stochastic linear programming. Grounded on the preliminaries in Section 2.2.2, we presented the setups of the master problem and subproblems.

To better represent the randomness intrinsic to the planning period, we chose GMM to form smooth approximations to arbitrary PDFs of stochastic parameters in the distribution system. Therefore, based on the well-trained GMM, representative scenarios were generated via Monte Carlo sampling. Also, to fix the computational burden which increases with the scale of scenarios, we utilized two decomposition methods introduced in Section 2.3 to solve two-stage stochastic programming under the settings of 4, 20, 40, and 100 scenarios. By comparing the computation time of the L-shaped method and the PH algorithm, we demonstrated the superiority of the modified PH on efficiency in solving large-scale distribution system planning problems.

In order to make the best of PH algorithms' advantage in scenario-based decomposition, we implemented a paralleled PH algorithm. We also came up with two effective algorithmic enhancements and demonstrated their effectiveness by four different PH algorithms. In the convergence profile of each PH algorithm, the modified PH outperforms the basic PH, the average-solution PH, and the gap-dependent PH. This corroborates the significance of combining enhancements proposed in Sections 4.3.3.1 and 4.3.3.3.

CHAPTER 5 CONCLUSIONS AND FUTURE WORK

5.1 Dissertation Summary

In this dissertation, both regulation services and degradation penalty of ESSs were considered to minimize the overall planning cost of distribution systems. The planning decision of line configuration, substation expansion, storage siting and sizing on the 33-bus distribution network is optimized via a MILP model. Subsequently, this deterministic model was reformulated to two-stage stochastic programming by adopting a GMM to handle various uncertainties. Then, a modified PH algorithm was proposed to solve the model with a parallel computing process, with which we improved the computation efficiency by 2-8 times compared with the Gurobi optimizer, and 3–15 times with the L-shaped method. Moreover, we observed from the deterministic planning results that adding degradation penalty to the objective can prolong the storage lifetime by one year, then cut down the overall cost during the whole planning.

Numerical results showed that ESSs earned as much revenue as energy arbitrage by offering regulation services. According to this finding, it is advised to promote the construction of storage units in distribution networks for higher profits. We were also noticed that the storage degradation over a planning horizon is necessary to be considered for applications to extend the lifespan of expensive ESSs. Besides, our modified PH algorithm was proved able to solve planning problems with multiple stochastic scenarios efficiently.

To demonstrate the effectiveness of each algorithmic enhancement of the modified PH algorithm, we performed controlled experiments on four different PH algorithms where they differ from each other on the use of the specific algorithmic enhancement. The result showed that though both enhancements can accelerate convergence when compared with the basic PH, computing a rational average solution is more effective in stable convergence. And the superiority of the modified PH further proved the effectiveness of combining two algorithmic enhancements.

Readers are encouraged to refer to https://doi.org/10.6084/m9.figshare.11952531.v1 for access to all datasets used in this dissertation. This is an open-sourced online data repository hosted by Figshare[79].

5.2 Future Work

We would also like to point out the work in progress as well as possible future works from the achievements of this dissertation. We bullet point the future directions on the formulation and solution of proposed DSEP models.

First, we can utilize mixed-integer second-order cone programming (MISOCP) for the distribution system planning that adopts the extended DistFlow model of AC-OPF[82]. By considering both active and reactive power flow, more ancillary services such as the voltage and reactive power support from ESSs can be modeled in the planning stage, thus further improving ESS financial value. At present, we have already implemented the MISOCP model on a 24-node test system[78]. Note that the integration of ESSs into the distribution system may lead to bi-directional power flow, the feasibility of planning results is supposed to be checked with AC power flow results.

On the other hand, the computational efficiency of the modified PH algorithm proposed in this dissertation can also apply to the above-mentioned MISOCP model. With more integer variables taken into account, new algorithmic enhancements are needed to ensure a fast convergence rate. To this end, we are now trying to implement the Frank-Wolfe progressive hedging (FW-PH) algorithm[83] to our planning model as the FW-PH is insensitive to the selection of iterative penalty factors. This characteristic also enables a wider range of FW-PH applications of stochastic optimization for distribution planning problems.

REFERENCES

[1]   IEA. Electricity market report - december 2020[J/OL]. Paris, 2020. https://www.iea.org/repo rts/electricity-market-report-december-2020.

[2]   Parra D, Norman S A, Walker G S, et al. Optimum community energy storage system for demand load shifting[J]. Applied Energy, 2016, 174: 130-143.

[3]   Shen X, Shahidehpour M, Han Y, et al. Expansion planning of active distribution networks with centralized and distributed energy storage systems[J]. IEEE Transactions on Sustainable Energy, 2016, 8(1): 126-134.

[4]   Blomgren G E. The development and future of lithium ion batteries[J]. Journal of The Electro-chemical Society, 2016, 164(1): A5019.

[5]   St John J. Report: Levelized cost of energy for lithium-ion batteries is plummeting[J]. Greentech Media, 2019.

[6]   Kloess M, Zach K. Bulk electricity storage technologies for load-leveling operation–an eco-nomic assessment for the austrian and german power market[J]. International Journal of Elec-trical Power & Energy Systems, 2014, 59: 111-122.

[7]   Zafirakis D, Chalvatzis K J, Baiocchi G, et al. The value of arbitrage for energy storage: Evi-dence from european electricity markets[J]. Applied energy, 2016, 184: 971-986.

[8]   Lazard L. Lazard's levelized cost of storage analysis, version 4.0[Z]. 2018.

[9]   Foggo B, Yu N. Improved battery storage valuation through degradation reduction[J]. IEEE Transactions on Smart Grid, 2017, 9(6): 5721-5732.

[10]   Saboori H, Hemmati R, Ghiasi S M S, et al. Energy storage planning in electric power distri-bution networks–a state-of-the-art review[J]. Renewable and sustainable energy reviews, 2017, 79: 1108-1121.

[11]   Oren S S. Design of ancillary service markets[C]// Proceedings of the 34th Annual Hawaii International Conference on System Sciences. IEEE, 2001: 9-pp.

[12]   Sioshansi F P. Evolution of global electricity markets: New paradigms, new challenges, new approaches[M]. Academic Press, 2013.

[13]   Andersson G, Donalek P, Farmer R, et al. Causes of the 2003 major grid blackouts in north amer-ica and europe, and recommended means to improve system dynamic performance[J]. IEEE transactions on Power Systems, 2005, 20(4): 1922-1928.

[14]   Kumar A, Meena N K, Singh A R, et al. Strategic integration of battery energy storage systems with the provision of distributed ancillary services in active distribution systems[J]. Applied Energy, 2019, 253: 113503.

[15]   Gan W, Ai X, Fang J, et al. Security constrained co-planning of transmission expansion and energy storage[J]. Applied energy, 2019, 239: 383-394.

[16] Geurin S O, Barnes A K, Balda J C. Smart grid applications of selected energy storage technologies[C]// 2012 IEEE PES Innovative Smart Grid Technologies (ISGT). IEEE, 2012: 1-8.

[17] Merten M, Olk C, Schoeneberger I, et al. Bidding strategy for battery storage systems in the secondary control reserve market[J]. Applied Energy, 2020, 268: 114951.

[18] Xu B, Oudalov A, Ulbig A, et al. Modeling of lithium-ion battery degradation for cell life assessment[J]. IEEE Transactions on Smart Grid, 2016, 9(2): 1131-1140.

[19] Xiaoping L, Ming D, Jianghong H, et al. Dynamic economic dispatch for microgrids including battery energy storage[C]// The 2nd international symposium on power electronics for distributed generation systems. IEEE, 2010: 914-917.

[20] Divya K, Østergaard J. Battery energy storage technology for power systems—an overview[J]. Electric power systems research, 2009, 79(4): 511-520.

[21] Han X, Lu L, Zheng Y, et al. A review on the key issues of the lithium ion battery degradation among the whole life cycle[J]. ETransportation, 2019, 1: 100005.

[22] Vetter J, Novák P, Wagner M R, et al. Ageing mechanisms in lithium-ion batteries[J]. Journal of power sources, 2005, 147(1-2): 269-281.

[23] Laresgoiti I, Käbitz S, Ecker M, et al. Modeling mechanical degradation in lithium ion batteries during cycling: Solid electrolyte interphase fracture[J]. Journal of Power Sources, 2015, 300: 112-122.

[24] Temraz H K, Quintana V H. Distribution system expansion planning models: an overview[J]. Electric Power Systems Research, 1993, 26(1): 61-70.

[25] Choi W S, Hwang S, Chang W, et al. Degradation of co 3 o 4 anode in rechargeable lithium-ion battery: a semi-empirical approach to the effect of conducting material content[J]. Journal of Solid State Electrochemistry, 2016, 20(2): 345-352.

[26] Park J, Appiah W A, Byun S, et al. Semi-empirical long-term cycle life model coupled with an electrolyte depletion function for large-format graphite/lifepo4 lithium-ion batteries[J]. Journal of Power Sources, 2017, 365: 257-265.

[27] Downing S D, Socie D. Simple rainflow counting algorithms[J]. International journal of fatigue, 1982, 4(1): 31-40.

[28] Cardoso G, Brouhard T, DeForest N, et al. Battery aging in multi-energy microgrid design using mixed integer linear programming[J]. Applied energy, 2018, 231: 1059-1069.

[29] He G, Chen Q, Kang C, et al. Optimal bidding strategy of battery storage in power markets considering performance-based regulation and battery cycle life[J]. IEEE Transactions on Smart Grid, 2015, 7(5): 2359-2367.

[30] Xi X, Sioshansi R. A dynamic programming model of energy storage and transformer deployments to relieve distribution constraints[J]. Computational Management Science, 2016, 13(1): 119-146.

[31] Berrada A, Loudiyi K, Zorkani I. Valuation of energy storage in energy and regulation markets[J]. Energy, 2016, 115: 1109-1118.

REFERENCES

[32] González-Garrido A, Gaztañaga H, Saez-de Ibarra A, et al. Electricity and reserve market bidding strategy including sizing evaluation and a novel renewable complementarity-based centralized control for storage lifetime enhancement[J]. Applied Energy, 2020, 262: 114591.

[33] Chen C, Sun H, Shen X, et al. Two-stage robust planning-operation co-optimization of energy hub considering precise energy storage economic model[J]. Applied energy, 2019, 252: 113372.

[34] Li Y, Vilathgamuwa M, Farrell T W, et al. Development of a degradation-conscious physics-based lithium-ion battery model for use in power system planning studies[J]. Applied Energy, 2019, 248: 512-525.

[35] Dong X, Yuying Z, Tong J. Planning-operation co-optimization model of active distribution network with energy storage considering the lifetime of batteries[J]. IEEE Access, 2018, 6: 59822-59832.

[36] Guerrero R C, Angelo M, Pedrasa A. An milp-based model for hybrid renewable energy system planning considering equipment degradation and battery lifetime[C]// 2019 IEEE 2nd International Conference on Power and Energy Applications (ICPEA). IEEE, 2019: 207-211.

[37] Gan L, Li N, Topcu U, et al. Exact convex relaxation of optimal power flow in radial networks[J]. IEEE Transactions on Automatic Control, 2014, 60(1): 72-87.

[38] Baran M E, Wu F F. Network reconfiguration in distribution systems for loss reduction and load balancing[J]. IEEE Power Engineering Review, 1989, 9(4): 101-102.

[39] Asensio M, de Quevedo P M, Muñoz-Delgado G, et al. Joint distribution network and renewable energy expansion planning considering demand response and energy storage—part i: Stochastic programming model[J]. IEEE Transactions on Smart Grid, 2016, 9(2): 655-666.

[40] Baringo L, Boffino L, Oggioni G. Robust expansion planning of a distribution system with electric vehicles, storage and renewable units[J]. Applied Energy, 2020, 265: 114679.

[41] Zhou Z, Zhang J, Liu P, et al. A two-stage stochastic programming model for the optimal design of distributed energy systems[J]. Applied Energy, 2013, 103: 135-144.

[42] Rafinia A, Moshtagh J, Rezaei N. Towards an enhanced power system sustainability: An milp under-frequency load shedding scheme considering demand response resources[J]. Sustainable Cities and Society, 2020: 102168.

[43] Reynolds D A. Gaussian mixture models.[J]. Encyclopedia of biometrics, 2009, 741.

[44] Ryan S M, Wets R J B, Woodruff D L, et al. Toward scalable, parallel progressive hedging for stochastic unit commitment[C]// 2013 IEEE Power & Energy Society General Meeting. IEEE, 2013: 1-5.

[45] Crainic T G, Hewitt M, Rei W. Scenario grouping in a progressive hedging-based meta-heuristic for stochastic network design[J]. Computers & Operations Research, 2014, 43: 90-99.

[46] Van Slyke R M, Wets R. L-shaped linear programs with applications to optimal control and stochastic programming[J]. SIAM Journal on Applied Mathematics, 1969, 17(4): 638-663.

[47] Rockafellar R T, Wets R J B. Scenarios and policy aggregation in optimization under uncertainty[J]. Mathematics of operations research, 1991, 16(1): 119-147.

[48] Birge J R, Louveaux F. Introduction to stochastic programming[M]. Springer Science & Business Media, 2011.

[49] Laporte G, Louveaux F V, Van Hamme L. An integer l-shaped algorithm for the capacitated vehicle routing problem with stochastic demands[J]. Operations Research, 2002, 50(3): 415-423.

[50] Biesinger B, Hu B, Raidl G. An integer l-shaped method for the generalized vehicle routing problem with stochastic demands[J]. Electronic Notes in Discrete Mathematics, 2016, 52: 245-252.

[51] Watson J P, Woodruff D L. Progressive hedging innovations for a class of stochastic mixed-integer resource allocation problems[J]. Computational Management Science, 2011, 8(4): 355-370.

[52] Liu Y, Sioshansi R, Conejo A J. Multistage stochastic investment planning with multiscale representation of uncertainties and decisions[J]. IEEE Transactions on Power Systems, 2017, 33(1): 781-791.

[53] Munoz F D, Watson J P. A scalable solution framework for stochastic transmission and generation planning problems[J]. Computational Management Science, 2015, 12(4): 491-518.

[54] Carvalho P M, Ferreira L A, Barruncho L. Hedging large-scale distribution system investments against uncertainty[C]// IEEE Power Engineering Society. 1999 Winter Meeting (Cat. No. 99CH36233): volume 2. IEEE, 1999: 901-906.

[55] Shen J, Dusmez S, Khaligh A. Optimization of sizing and battery cycle life in battery/ultracapacitor hybrid energy storage systems for electric vehicle applications[J]. IEEE Transactions on industrial informatics, 2014, 10(4): 2112-2121.

[56] Hamedi A S, Rajabi-Ghahnavieh A. Explicit degradation modelling in optimal lead–acid battery use for photovoltaic systems[J]. IET Generation, Transmission & Distribution, 2016, 10(4): 1098-1106.

[57] Zhao B, Zhang X, Chen J, et al. Operation optimization of standalone microgrids considering lifetime characteristics of battery energy storage system[J]. IEEE transactions on sustainable energy, 2013, 4(4): 934-943.

[58] Roh J H, Shahidehpour M, Wu L. Market-based generation and transmission planning with uncertainties[J]. IEEE Transactions on Power Systems, 2009, 24(3): 1587-1598.

[59] Domínguez R, Conejo A J, Carrion M. Toward fully renewable electric energy systems[J]. IEEE Transactions on Power Systems, 2014, 30(1): 316-326.

[60] López J A, Ponnambalam K, Quintana V H. Generation and transmission expansion under risk using stochastic programming[J]. IEEE Transactions on Power systems, 2007, 22(3): 1369-1378.

[61] Aien M, Hajebrahimi A, Fotuhi-Firuzabad M. A comprehensive review on uncertainty modeling techniques in power system studies[J]. Renewable and Sustainable Energy Reviews, 2016, 57: 1077-1089.

[62] Soroudi A. Possibilistic-scenario model for dg impact assessment on distribution networks in an uncertain environment[J]. IEEE Transactions on Power Systems, 2012, 27(3): 1283-1293.

[63] Singh C, Kim Y. An efficient technique for reliability analysis of power systems including time dependent sources[J]. IEEE Transactions on Power Systems, 1988, 3(3): 1090-1096.

[64]   Allan R, Da Silva A L, Burchett R. Evaluation methods and accuracy in probabilistic load flow solutions[J]. IEEE Transactions on Power Apparatus and Systems, 1981(5): 2539-2546.

[65]   Papaefthymiou G, Kurowicka D. Using copulas for modeling stochastic dependence in power system uncertainty analysis[J]. IEEE Transactions on Power Systems, 2008, 24(1): 40-49.

[66]   Birge J, Louveaux F. L-shaped method for two-stage stochastic programs with recourse[M]// Encyclopedia of Optimization 2009: CA Floudas, PM Pardalos, editors. 2009: 1943-1945.

[67]   Dantzig G B. Linear programming under uncertainty[J]. Management science, 1955, 1(3-4): 197-206.

[68]   Beale E M. On minimizing a convex function subject to linear inequalities[J]. Journal of the Royal Statistical Society: Series B (Methodological), 1955, 17(2): 173-184.

[69]   Carøe C C, Tind J. L-shaped decomposition of two-stage stochastic programs with integer recourse[J]. Mathematical Programming, 1998, 83(1): 451-464.

[70]   Laporte G, Louveaux F V. The integer l-shaped method for stochastic integer programs with complete recourse[J]. Operations research letters, 1993, 13(3): 133-142.

[71]   Gade D, Hackebeil G, Ryan S M, et al. Obtaining lower bounds from the progressive hedging algorithm for stochastic mixed-integer programs[J]. Mathematical Programming, 2016, 157(1): 47-67.

[72]   Abdulgalil M A, Khalid M. Enhancing the reliability of a microgrid through optimal size of battery ess[J]. IET Generation, Transmission & Distribution, 2019, 13(9): 1499-1508.

[73]   Mohd A, Ortjohann E, Schmelter A, et al. Challenges in integrating distributed energy storage systems into future smart grid[C]// 2008 IEEE international symposium on industrial electronics. IEEE, 2008: 1627-1632.

[74]   Wankmüller F, Thimmapuram P R, Gallagher K G, et al. Impact of battery degradation on energy arbitrage revenue of grid-level energy storage[J]. Journal of Energy Storage, 2017, 10: 56-66.

[75]   Haffner S, Pereira L F A, Pereira L A, et al. Multistage model for distribution expansion planning with distributed generation—part i: Problem formulation[J]. IEEE Transactions on Power Delivery, 2008, 23(2): 915-923.

[76]   Haffner S, Pereira L F A, Pereira L A, et al. Multistage model for distribution expansion planning with distributed generation—part ii: Numerical results[J]. IEEE Transactions on Power Delivery, 2008, 23(2): 924-929.

[77]   Lotero R C, Contreras J. Distribution system planning with reliability[J]. IEEE Transactions on Power Delivery, 2011, 26(4): 2552-2562.

[78]   Muñoz-Delgado G, Contreras J, Arroyo J M. Joint expansion planning of distributed generation and distribution networks[J]. IEEE Transactions on Power Systems, 2014, 30(5): 2579-2590.

[79]   Zhao X, Shen X. Dataset for stochastic planning of distribution system considering ess regulation services and degradation[M/OL]. figshare, 2020. https://figshare.com/articles/Dataset_fo r_Stochastic_Planning_of_Distribution_System_Considering_ESS_Regulation_Services_and _Degradation/11952531/1. DOI: 10.6084/m9.figshare.11952531.v1.

[80] Foggo B. Replication Data for: Battery Storage Valuation with Optimal Degradation[M/OL]. Harvard Dataverse, 2016. https://doi.org/10.7910/DVN/KDHAJY.

[81] Bontemps C, Meddahi N. Testing normality: a gmm approach[J]. Journal of Econometrics, 2005, 124(1): 149-186.

[82] Farivar M, Low S H. Branch flow model: Relaxations and convexification—part i[J]. IEEE Transactions on Power Systems, 2013, 28(3): 2554-2564.

[83] Boland N, Christiansen J, Dandurand B, et al. Combining progressive hedging with a frank–wolfe method to compute lagrangian dual bounds in stochastic mixed-integer programming[J]. SIAM Journal on Optimization, 2018, 28(2): 1312-1336.

ACKNOWLEDGEMENTS

声　明

本人郑重声明：所呈交的学位论文，是本人在导师指导下，独立进行研究工作所取得的成果。尽我所知，除文中已经注明引用的内容外，本学位论文的研究成果不包含任何他人享有著作权的内容。对本论文所涉及的研究工作做出贡献的其他个人和集体，均已在文中以明确方式标明。

签　名：赵心怡　日　期：2021年5月25日

RESUME

Xinyi Zhao was born July 24, 1996 in Wuhan city, Hubei province.

In September 2014, she was admitted to the College of Electrical Engineering at Wuhan University. In July 2018, she graduated with a Bachelor of Engineering degree.

In September 2018, she was admitted to Tsinghua-Berkeley Shenzhen Institute (TBSI) at Tsinghua University for a Master of Science degree in Environmental Science and New Energy Technology.

Published Papers

[1] **Xinyi Zhao**, Xinwei Shen, Qinglai Guo, Hongbin Sun and Shmuel S. Oren. A Stochastic Distribution System Planning Method Considering Regulation Services and Energy Storage Degradation[J]. Applied Energy, 2020, 277:115520. (SCI)

[2] **Xinyi Zhao**, Xinwei Shen, Hongkun Chen, et al. A Two-Stage Multi-Objective Planning Strategy for Electric Vehicle Charging Stations Considering Power-loss Sensitivity in Distribution System[C]. 2nd IEEE Conference on Energy Internet and Energy System Integration, 2018. (EI)

[3] **Xinyi Zhao**, Xinwei Shen, Tian Xia, et al. Optimal Distribution System Planning Considering Regulation Services and Degradation of ESSs[C]. 11th International Conference on Applied Energy, 2019. (EI)

[4] Yuquan Liu, **Xinyi Zhao**, Xinwei Shen, et al. A Distribution System Expansion Planning Method Considering Integrated Energy Service Providers' Revenue on Energy Storage Investment[C]. 5th International Conference on Electricity Distribution, 2019. (EI)

Patents

[5] **赵心怡**, 尹琳鑫, 宋师男, 胡慧怡, 张治, 郑宇. 一种基于六轴加速度传感器的人体膝反射智能诊疗叩诊锤: 中国, CN106943161B[P]. 2020-02-11.

COMMENTS FROM THESIS SUPERVISOR

This dissertation discusses and explores the power distribution system (PDS) expansion planning problem with energy storage (ES) providing ancillary service (AS), e.g. energy arbitrary and frequency regulation service for PDS, which is considered to be an important future trend of ES's application in smart grid. It proposes a stochastic planning method to address PDS's uncertainties in terms of renewable and load fluctuations, as well as AS prices, in which a scenario-based decomposition method, i.e. progressive hedging (PH), is modified and applied to accelerate the convergence and even outperform state-of-the-art commercial software in case studies. This dissertation is overall well-structured, with sufficient literature review and research gap concluded in the introduction, followed by theory preliminaries. Then the deterministic planning model is proposed for PDS planning with ES considering its AS benefits and degradation cost, and further developed to be a two-stage stochastic programming model and solved by modified PH, showing its clear contributions to the related research area.

COMMENTS FROM THESIS SUPERVISOR GROUP

This dissertation focused on the distribution system expansion planning with energy storage systems. The degradation of storage units together with their provision of ancillary services is co-optimized in mixed-integer linear programming. The author made a synthetic review of the relevant literature and had solid contributions to both model formulation and acceleration algorithm. Besides, it is noted that she published one paper in a top-tier journal and three papers at international conferences during graduate study. Grounded on her achievements and the dissertation content, we agree that she is ready to submit the dissertation and will be qualified for an MS degree by the defense.

RESOLUTION OF THESIS DEFENSE COMMITTEE

The dissertation proposes an expansion planning model for distribution systems with energy storage systems (ESSs) where the storage degradation and ancillary service revenue are both considered. The proposed model is formulated as mixed-integer linear programming that optimizes the overall planning cost, including investment and maintenance cost, power transaction cost and ESS revenue from frequency regulation ancillary services. A degradation penalty is added to the objective to avoid excessive charge/discharge when ESS provides ancillary services, thus prolonging its lifespan to make more profits.

Main innovative achievements of this dissertation include：

1. A two-stage stochastic planning model for power distribution systems considering ESS degradation is proposed, where energy arbitrage and frequency regulation services provided by ESSs are co-optimized with ESSs' siting and sizing options.

2. We leverage a Gaussian mixture model to better illustrate the uncertainty in the distribution system for scenario generation instead of directly sampling uncertain parameters from their historical data.

3. A modified progressive hedging (PH) algorithm with parallel computing is introduced to improve the computation efficiency. Based on the traditional PH algorithm, the idea of implementing *non-anticipativity* constraints by computing a rational average solution instead of the mathematical expectation is originally presented. Moreover, with gap-dependent penalty factors, the modified PH algorithm is further improved in solving the proposed model and has outperformed a solver Gurobi and the L-shaped method.

This thesis demonstrated that the candidate has acquired solid fundamental knowledge and systematic specific research knowledge in relevant disciplines, ability to comprehensively combine his/her knowledge to carry out original, pioneering and interdisciplinary research or independently undertake specialized technical work. The dissertation is of clear structure, exhibited a rigorous logic and conformed to the standard format for presentation of figures and tables. During the defense, the candidate presented the thesis appropriately and addressed the questions in a satisfactory manner. Through an anonymous ballot, the five members of the defense committee voted unanimously to recommend that Xinyi Zhao be awarded a master's degree.